6.0 References

1. I. Hamerton, ed., Chemistry and Technology of Cyanate Ester Resins, 1st Ed., Wiley-Interscience, New York, (1995).
2. S. A. Srinivasan, Ph.D. Dissertation, Virginia Tech, 1994.
3. F. W. Billmeyer, Jr., Textbook of Polymer Science, 3rd Ed., Wiley-Interscience, New York, (1984).
4. Houben-Weyl, Methoden der Organischen Chemie, **vol.8**, 3 thieme, Stuttgart, pp. 89 and 125, (1952).
5. T. Sandmeyer, Ber. dtsch. chem. Fes., **19**, 862, (1886).
6. S. Cloez, C. R. hebd. Seances Acad. Sci. **44**, 482, (1857).
7. E. Grigat, R. Putter, German Patent 1195764, Farben-fabriken, Bayer AG, (Feb. 16th, 1963).
8. E. Grigat, R. Putter, German Patent 1201839, Farben-fabriken, Bayer AG, (Feb. 7th, 1963).
9. E. Grigat, R. Putter, Chem. Ber., **97**, 3012, (1964).
10. D. Martin, Agnew. Chem. internat. ed., **3**, 311, (1964).
11. K. A. Jensen, A. Holm, Acta. Chem. Scand., **18**, 826, (1964)
12. E. Grigat, R. Putter, Agnew. Chem. internat. ed., **vol.6**,3,p. 206, (1967).
13. D. Martin, A. Weise, Chem. Ber., **99**, 976, (1965).
14. D. Martin, Agnew. Chem. internat. ed., **4**, 985, (1965).
15. M. Hedayatullah, L. Denivelle, C. R. hebd. Seances Acad. Sci., **256**, 4029, (1963).

16. E. Grigat, R. Putter, Chem. Ber., **97**, 3018, (1964).

17. E. Grigat, R. Putter, German Patent 1183507, Farben-fabriken, Bayer AG, (May 2nd, 1963).

18. D. A. Shimp, J. R. Christenson, S. J. Ising, 'AroCy Cyanate Ester Resins: Chemistry and Properties', Rhone-Poulenc, Inc. publication, (1989).

19. E. Grigat, R. Putter, USP 3, **553**, 244, Jan. 5th, (1971).

20. D. A. Shimp, SAMPE Quarterly, October, p. 41, (1987).

21. S. J. Ising, Proc. of IPC Fall Meeting, Anaheim, California, Oct. 23-25, (1988).

22. D. A. Shimp, Proc. of 34th SAMPE Symp. & Exhib., Reno, Nevada, May 8-11, (1989).

23. G. W. Bogan, SAMPE Journal, **vol. 24**(6), Nov/Dec, (1988).

24. D. A. Jarvie, 33rd Int'l SAMPE Symp., March 7-10, 1405, (1988).

25. S. Das, D. C. Preorsek, USP 4, **831**, 086, May (1989).

26. S. Das, D. C. Preorsek, B. T. DeBona, Mod. Plast., p. 72, Feb. (1990).

27. S. Das, D. C. Preorsek, B. T. DeBona, 21st Int'l SAMPE Tech. Conf., Sept. 25-28, p. 972, (1989).

28. J. C. Abed, J. E. McGrath, ACS Polym. Mat. Sc. & Eng., **vol. 69**, 291, (1993).

29. J. C. Abed, R. Mercier, S. A. Srinivasan, J. E. McGrath, ACS Polym. Prepr., Div. of Polym. Chem., **33**(2), 233, (1992).

30. D. A. Shimp, J. R. Christenson, S. J. Ising, ACS Polym. Mat. Sc. & Eng., **vol. 66**, 292, (1992).

31. H. D. Stenzenberger in 'Polyimides', D. Wilson, H. D. Stenzenberger, P. Hergenrother, eds., Blackie, Glasgow, UK, (1991).

32. J. M. Barton, I. Hammerton, J. R. Jones, Polymer Int'l, **29**, 145, (1992).

33. G.G. Barclay, C. K. Ober, K. I. Papathomas, D. W. Wang, Macromolecules, **25**, 2947, (1992).

34. D. A. Shimp, J. E. Wentworth, 37th Int'l SAMPE Symp., March 9-12, p. 293, (1992).

35. To Bayer AG USP 3, **562**, 214, Feb. 9, (1971).

36. M. Bauer, J. Bauer, R. Ruhmann, G. Kuhn, Acta Polymerica, **40**(6), 397, (1989).

37. C. A. Fyfe, J. Niu, S. J. Rettig, N. E. Burlinson, C. M. Reidsema, D. W. Wang, M. Poliks, Macromolecules, **25**, 6289, (1992).

38. A. Osei-Owusu, G. C. Martin, J. T. Gotro, Polym. Eng. & Sci., **31** (22), 1604, (1991).

39. A. Osei-Owusu, G. C. Martin, J. T. Gotro, Polym. Eng. & Sci., **32** (8), 535, (1992).

40. A. M. Gupta, Macromolecules, **24**, 3459, (1991).

41. M. Bauer, J. Bauer, G. Kuhn, Acta Polymerica, **37**, 715, (1986).

42. J. Bauer, P. Lang, W. Burchard, M. Bauer, Macromolecules, **24**(9), 2654, (1991).

43. D. A. Shimp, J. R. Christenson, S. J. Ising, 3rd Int'l SAMPE Electronic Materials & Process Conf., **vol. 3**, p. 360, (1989).

44. S. L. Simon, J. K. Gillham, D. A. Shimp, ACS Polym. Mat. Sci. & Eng., **62**, 96, (1990).

45. J. M. Barton, D. C. L. Greenfield, I. Hammerton, J. R. Jones, Polym. Bull., **25**, 475, (1991).

46. A. M. Gupta, C. W. Macosko, Makromol. Chem. Macromol. Symp., **45**, 105, (1991).

47. A. M. Gupta, C. W. Macosko, Macromolecules, **26**, 2455, (1993).

48. R. J. J. Williams, A. Vazquez, J. P. Pascault, Polym. Bull., **28**, 219, (1992).

49. S. Zeng, M. Horsington, J. Seferis, D. A. Shimp, 37th Int'l SAMPE Symp., March 9-12, p. 348, (1992).

50. P. C. Yang, D. M. Pickelman, E. P. Woo, 35th Int'l SAMPE Symp., April 2-5, p. 1131, (1990).

51. P. C. Yang, E. P. Woo, S. A. Laman, J. J. Jakubowski, D. M. Pickelman, H. S. Sue, 36th Int'l SAMPE Symp., April 15-18, p. 431, (1991).

52. C. Arnold, P. Mackenzie, V. Malhorta, D. Pearson, N. Chow, M. Hearn, G. Robinson, 37th Int'l SAMPE Symp., March 9-12, p. 128, (1992).

53. G. Almen, P. Mackenzie, V. Malhorta, E. Maskell, 35th Int'l SAMPE Symp., March 9-12, p. 128, (1992).

54. G. R. Almen, SAMPE Int'l Tech. Conf., **21**, 304, (1989).

55. D. A. Shimp, F. A. Hudock, W. S. Bobo, 18th Int'l SAMPE Tech. Conf., Oct. 7-9, p. 851, (1986).

56. Z. Q. Cao, F. Mechin, J. P. Pascault, Polym. Mater. Sci. Eng. (PMSE) Prepr., **vol. 70**, p. 91, (1994).

57. J. C. Hedrick, A. Viehbeck, J. T. Gotro, ACS Polym. Prepr., Polym. Chem., **vol. 35**(1), p. 537, March, (1994).

58. S. A. Srinivasan, J. E. McGrath, SAMPE Quarterly, **24**(3), 25, (1993).

59. S. A. Srinivasan, J. C. Abed, J. E. McGrath, ACS Polym. Prepr., Polym. Chem., **vol**. **33**(2), p. 325, March, (1992).

60. S. A. Srinivasan, G. D. Lyle, J. E. McGrath, 38th International SAMPE Symp., Anaheim, California, p. 28, May, (1993).

61. S. A. Srinivasan, J. E. McGrath, High Performance Polymers, **vol. 5**, pp. 259-274, (1993).

62. S. A. Srinivasan, J. E. McGrath, Proc. of the 9th Int'l Conf. on Composite Materials, Antonio Miravete, ed., July 12-16, Madrid, Spain, p.875, (1993).

63. S. A. Srinivasan, S. S. Joardar, D. B. Priddy, Jr., T. C. Ward, J. E. McGrath, 39th International SAMPE Symp and Exhib., Anaheim, California, April, (1994).

64. S. A. Srinivasan, S. S. Joardar, D. B. Priddy, Jr., T. C. Ward, J. E. McGrath, Materials Research Society, Spring Meeting, San Francisco, California, April, (1994).

65. S. A. Srinivasan, S. S. Joardar, D. B. Priddy, Jr., T. C. Ward, J. E. McGrath, Polym. Mat. Sci. Eng. (PMSE) Prepr., **vol. 70**, p. 93, (1994).

66. S. E. B. Petrie, in Polymeric Materials: Relationships Between Structure and Mechanical Behavior, Am. Soc. for Metals, Metal Park, Ohio (1975).

67. A. J. Kovacs, J. M. Hutchinson, J. J. Aklonis, in The Structure of Non-Crystalline Materials, P. H. Gaskell, Ed., Taylor & Francis, London (1977).

68. L. C.E. Struik, Polym. Eng. Sci., **17**, 165 (1977).

69. M. R. Tant, G. L. Wilkes, Polym. Eng. Sci., **21**, 14, 874 (1981).

70. L. C.E. Struik, Physical Aging in Amorphous Polymers and Other Materials., Elsevier, Amsterdam (1978).

71. L. C.E. Struik, Internal Stresses, Dimensional Instabilities and Molecular Orientations in Plastics, John Wiley and Sons, New York (1990).

72. G. Hamed, Elastomerics, **120**, 14 (1988).

73. M. W. Muggli, Ph.D. Dissertation, Virginia Tech, 1998.

74. I. M. Ward, Mechanical Properties of Solid Polymers, Wiley-Interscience, New York (1971).

75. J. D. Ferry, Viscoelastic Properties of Polymers, Wiley & Sons, New York (1971).

76. R. B. Bird, W. E. Stewart, E. N. Lightfoot, Transport Phenomena, Wiley & Sons, New York (1971).

77. M. L. Williams, J. Phys. Chem., **59**, 95 (1955).

78. A. K. Doolittle, J. Appl. Phys., **22**, 1471 (1951)

79. M. L. Williams, R. F. Landel, J. D. Ferry, J. Am. Chem. Soc., **77**, 3701 (1955).

80. M. H. Cohen, D. Turnbull, J. Chem. Phys., **31**, 1164 (1959).

81. D. Turnbull, M. H. Cohen, J. Chem. Phys., **34**, 120 (1961).

82. J. H. Gibbs, E. A. DiMarzio, J. Chem. Phys., **28**, 373 (1958).

83. J. H. Gibbs, E. A. DiMarzio, J. Chem. Phys., **28**, 807 (1958).

84. G. Adam, J. H. Gibbs, J. Chem. Phys., **43**, 139 (1965).

85. P. Ehrenfest, Proc. Kon. Akad. Wetensch, Amsterdam, **36**, 153 (1933).

86. G. Rehage, W. Borchard, The Physics of Glassy Polymers, Wiley & Sons, New York (1973).

87. S. L. Rosen, Fundemental Principles of Polymeric Materials, Barnes & Noble, New York (1971).

88. S. Matsuoka, H. E. Bair, S. S. Bearder, H. E. Kern, J. T. Ryan, Polym. Eng. Sci., **18**, 1073 (1978).

89. Z. H. Ophir, J. A. Emerson, G. L. Wilkes, J. Appl. Phys., **49**, 5032 (1978).

90. M. van Gurp, J. Palmen, Rheology Bull., **67**, 1, 5 (1998)

91. D. J. Plazek, J. Rheol., **40**, 987 (1996)

92. D. L. Hunston, W. T. Carter, J. L. Rushford, "Linear Viscoelastic Properties of Solid Polymers as Modeled by a Simple Epoxy, Developments in Adhesives, 2, 125-172 (1981)

93. F. R. Schwarzl, F. Zahradnik, Rheol. Acta, **19**, 137 (1980).

94. Y. Diamant & M. Folman, Polymer, **20**, 1025 (1979).

95. M. Sumita, T. Shizuma, K. Miyasaka, K. Ishikawa, J. Macromol. Sci.: Phys., **B22**, 601 (1983)

96. J. M. Crissman, G. B. McKenna, J. Polym. Sci.: Polym. Phys., **28**, 1463 (1990).

97. R. Pixa, C. Goett, D. Froelich, Polym. Bull. (Berlin), **14**, 53 (1985).

98. G. B. McKenna, A. J. Kovacs, Polym. Prepr. (Am. Chem. Soc. Div. Polym. Chem.), **24**, 100 (1983).

99. A. J. Kovacs, Fortschr. Hochpolym. Forsch, **3**, 394 (1964).

100. J. Y. Cavaille, S. Etienne, J. Perez, L. Monnerie, G. P. Johari, Polymer, **27**,686 (1986).
101. D. J.Plazek, Z. N. Frund, Jr., J. Polym. Sci., Polym. Phys., **28**, 431 (1990).
102. M. G. Wyzgoski, J. Appl. Polym. Sci., **25**, 1455 (1980).
103. J. M. G. Cowie, R. Ferguson, Macromolecules, **22**, 2312 (1989).
104. D. J. Kemmish, J. N. Hay, Polymer, **26**, 905 (1985).
105. M. G. Wyzgoski, J. Appl. Polym. Sci., **25**, 1455 (1980).
106. W. H. Jo, K. J. Ko, Polym. Eng. Sci., **31**, 239 (1991).
107. A. Aref-Azar, J. N. Hay, Polymer, **23**, 1127 (1982).
108. Relaxation Phenomena in Polymers, Matsuoka S., Ed., Hanser Publishers, Munich, 1992
109. B. E. Read, J. Non-Cryst. Solids, **131-133**, 408 (1991).
110. L. C. E. Struik, Polymer, **28**, 1521 (1987).
111. L. C. E. Struik, Polymer, **28**, 1534 (1987).
112. L. C. E. Struik, Polymer, **30**, 799 (1989).
113. L. C. E. Struik, Polymer, **30**, 815 (1989).
114. J. C. Arnold, J. Polym. Sci., Part B: Polym. Phys., **31**, 1451 (1993).
115. M. E. Nichols, S. S. Wang, P. H. Geil, J. Macromol. Sci., Phys., **B29**, 303 (1990).
116. H. Parvatareddy, J. Z. Wang, D. A. Dillard, T. C. Ward, Comp. Sci and Tech., **53**, 4, 399 (1995)
117. C. G. Sell, G. B. McKenna, Polymer, **33**, 2103 (1992).
118. F. H. J. Maurer, J. H. M. Palmen, H. C. Booij, Rheol Acta, **24**, 243 (1985).

119. J. Mijovic, S. T. Devine, T. Ho, J. Appl. Polym. Sci., **39**, 1133 (1990).

120. M. G. Wyzgoski, J. Appl. Polym. Sci., **25**, 1443 (1980).

121. S. A. Schwartz, R. Bubeck, Polym. Eng. Sci.,**28**, 1 (1988).

122. A. Espinoza, J. J. Aklonis, Polym. Eng. Sci., **33**, 486 (1993).

123. G. B. McKenna, A. J. Kovacs, Polym. Prepr. (Am. Chem. Soc. Div. Polym. Chem.), **24**, 100 (1983).

124. S. L. Simon, J. K. Gillham, Polym. Mater. Sci. Eng., **66**, 277 (1992).

125. W. H. Jo, K. J. Ko, Polym. Eng. Sci., **31**, 239 (1991).

126. J. Y. Cavaille, S. Etienne, J. Perez, L. Monnerie, G. P. Johari, Polymer, **27**,686 (1986).

127. R. Pixa, C. Goett, D. Froelich, Polym. Bull. (Berlin), **14**, 53 (1985).

128. L. Guerdoux, E. Marchal, Polymer, **22**, 1199 (1981).

129. J. S. Royal, J. M. Torkelson, Macromolecules, **26**, 5331 (1993).

130. J. S. Royal, J. M. Torkelson, Macromolecules, **23**, 3536 (1990).

131 D. C. McHerron, G. L. Wilkes, Polym. Prepr. (Am. Chem. Soc. Div. Polym. Chem.), **33**, 1142 (1992).

132. D. C. McHerron, G. L. Wilkes, Polymer, **34**, 915 (1993).

133. D. J. Carlsson,D. M. Wiles, in J. I. Kroschwitz ed., Encyclopedia of Polymer Science and Engineering, John Wiley & Sons, New York, (1985) **Vol. 4**, p. 630.

134. D. J. Carlsson and D. M. Wiles, in ref. 133, vol 3, p.646.

135. J. M. Widmaier, J. P. Balmer, G. C. Meyer, Polym. Mater. Sci. Eng., **56**, 96 (1987).

136. C. D. Doyle, J. Appl. Polymer Sci., **6**, 638 (1962).

137. T. Ozawa, Ball, Chem. Soc. Jap., **38**, 1881 (1965)

138. J. H. Flynn, and L. A. Wall, Polymer Letters, **4**, 323 (1966).

139. A. Blaga, R. S. Yamasaki, J. Mater. Sci, **11**, 1513 (1976).

140. G. T. Merral, A. C. Meeks, J. Appl. Polym. Sci., **16**, 3389 (1972).

141. G. A. George, R. E. Sacher, J. F. Sprouse, J. Appl. Polym. Sci., **8**, 2241 (1977).

142. V. Bellinger, C. Bouchard, P. Claveirolle, J. Verdu, Polym. Photochem., **1**,69 (1977).

143. S. C. Lin, B. J. Bulkin, E. M. Pearce, J. Polym. Sci., Polym. Chem. Ed., **17**, 3121 (1979).

144. V. Bellinger, J. Verdu, J. Appl. Polm. Sci., **30**, 363 (1985).

145. A. Davis, Polym. Deg. Stab., **3**, 187 (1981).

146. N. Grassie and R. S. Roche, Makromol. Chem., **112**, 34 (1968).

147. O. Nishimura and Z. Ozawa, Polym. Photochem., **1**, 191 (1981).

148. V. Reinohl, J. Sedlar and M. Navratil, Polym. Photochem., **1**, 163 (1981).

149. N. Grassie and R. S. Roche, Makromol. Chem., **112**, 16 (1968).

150. A. Holstrom, A. Andersson and E. M. Sorvik, Eur. Polym. J., **13**, 483 (1977).

151. D. L. Allara and C. W. White, Adv. Chem. Ser., **169**, 273 (1978).

152. P. P. Klemchuk, Polym. Photochem., **3**, 1 (1983).

153. N. S. Allen, ed., Degradation and Stabilization of Polyolefins, Applied Science Publishers, Ltd., London, 1983 p. 337.

154. S. G. Hong, T. C. Wang, J. Appl. Polym. Sci., **52**, 1339 (1994).

155. S. S. Stivala, J. Kimura and S. M. Gabay, in ref. 148, p. 63.

156. N. C. Billingham and P. D. Calvert in ref 148, p.1.

157. G. Geuskens and M. S. Kabamba, Polym. Deg. Stab., **5**, 399 (1983).

158. R. H. Stille, Dev. Polym. Deg., **1**, 11 (1977).

159. I. C. McNeill, Dev. Polym. Deg., **1**, 43 & 171 (1977).

160. N. C. Billingham, D. C. Bott and A. S. Manke, Polym. Deg., **3**, 63 (1981).

161. J. L. Koenig, Adv. Polym. Sci., **54**, 87 (1983).

162. D. J. Carlsson, L. H. Gan and D. M. Wiles, J. Polym. Sci.; Polym. Chem. Ed.,**16**, 2365 (1978).

163. G. D. Mendenhall, Angew. Chem. Int. Ed. Engl., **16**, 225 (1977).

164. G. A. George, Dev. Polym. Deg., **3**, 173 (1981).

165. D. J. Carlsson and D. M. Wiles, Macromolecules, **4**, 174, 179 (1971).

166. P. Blais, M. Day and D. M. Wiles, J. Appl. Polym. Sci., **17**, 1895 (1973).

167. D. J. Carlsson and D. M. Wiles, Macromolecules, **2**, 597 (1969).

168. D. J. Carlsson and S. M. Milnera, J. Appl. Polym. Sci., **27**, 1589 (1982).

169. R. B. Larrabee, E. M. Barrall, II, C. D. Snyder, F. Levy, W. W. Fleming, Polym. Mater. Sci. Eng., **58**, 527 (1988).

170. F. A. Bovay, F. C. Schilling and H. N. Cheng, Adv. Chem. Ser., **169**, 133 (1978).

171 D. J. Carlsson and D. M. Wiles, in ref. 133, vol 4, p.691.

172. H. E. Baer, in E. A. Turi, ed., Thermal Characterization of Polymeric Materials, Academic Press, Inc., New York, 1981, p. 845.

173. J. B. Howard and H. M. Gilroy, Polym. Eng. Sci., **15**, 268 (1975).

174. H. Leaderman,Elastic and Creep Properties of Filamentous Materials and Other High Polymers, The Textile Foundation, Washington, 1943

175. A. V. Tobolsky, E. Catsiff, J. Polym. Sci., **19**, 111 (1956)

Appendix A DEVELOPMENT OF MEASUREMENT METHODS FOR CURE PROPERTIES USING DYNAMIC MECHANICAL ANALYSIS

A.1 LITERATURE REVIEW

A.1.1 Time-Temperature-Transformation (TTT) Diagrams

Theory and Development

A time-temperature-transformation (TTT) isothermal cure diagram is an excellent method for understanding the cure and physical behavior in thermosetting materials[A1 - A3]. Relationships between these variables influence the ultimate properties of a material. The main features of a TTT diagram are obtained by following the times when certain curing events occur over a family of isothermal cures, and which occur over a range of cure temperatures. These features include gelation, vitrification, “full cure”, de-vitrification and phase separation (two-phase systems) and are represented in Figure A1.

Chemical reactions during a thermosetting cure yield distinct states, as represented in Figure A1. These states include the sol/glass, liquid, sol/gel rubber, gel rubber (elastomer), ungelled sol glass, gelled glass, and char regions.

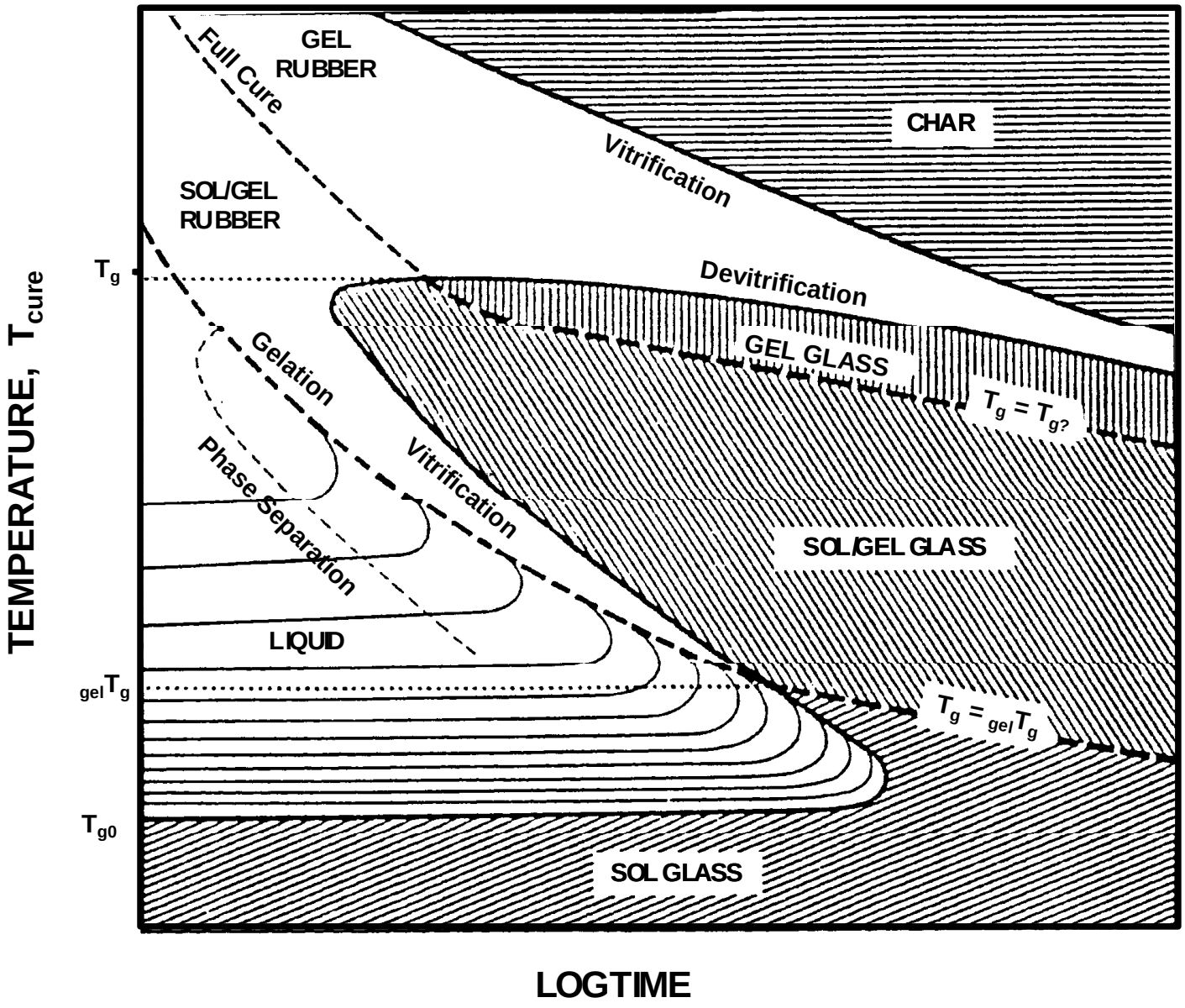

Figure A1. Time-Temperature-Transformation (TTT) isothermal cure diagram for a thermosetting system.(A2)

The sol glass region is characterized as the region below T_{g0}, the glass transition of the freshly mixed uncured resin, and essentially no reaction occurs in this region because the reactive species are immobilized in the glassy state.

The liquid region is represented as the region above T_{g0}, but below $T_{g\infty}$, and is bounded by the vitrification of the material. Flow and viscosity properties in this region tend to behave as in normal liquids[A4]. The gel/glass region is divided into two sections by the full-cure line. In the absence of degradation (de-vitrification and char), the upper and lower parts of this region are designated as the fully cured gel/glass and the under cured sol/gel glass regions, respectively. The processing terms, A-, B-, and C-stage resins correspond to sol/glass, sol/gel glass and fully cured gel/glass regions, respectively. The diagram also displays the transition temperatures $T_{g\infty}$, ${}_{gel}T_g$, and T_{g0}, which are determined by cure. They are the glass transition of the fully cured system, the temperature at which gelation and vitrification occur simultaneously, and the glass temperature of the reactants, respectively. A series of zero shear-rate, iso-viscous contours are included in the liquid region of the illustration. Each successive contour differs by a factor of ten[A4] and represents the viscosity (proportional to reaction rate) as the cure proceeds. The vitrification process below ${}_{gel}T_g$ has been constructed to be an iso-viscous curve.

Gelation of a material occurs when an infinite molecular network is formed. This formation produces long range elastic behavior in the liquid state, and the molecular weight and the zero shear-rate viscosity become infinite. The result is

that macroscopic flow and the growth of a dispersed phase (two-phase systems) is impeded. When gelation occurs, two distinct fractions are formed: the sol (solvent soluble) and the gel (solvent insoluble). After gelation has occurred, the ratio of sol to gel decreases with increasing conversion. The T_g of a system at a composition corresponding to gelation is ${}_{gel}T_g$, since gelation occurs as the system vitrifies when $T_{cure} = {}_{gel}T_g$ [A5]. The gelation curve corresponds to T_g equal to ${}_{gel}T_g$. This temperature is important in determining the upper temperature for storing reactive materials, since avoiding gelation is crucial for processing of such a resin.

Vitrification occurs when the T_g of the material advances to the isothermal cure temperature. The material is liquid or rubbery when the cure temperature is greater than T_g and glassy when T_g is greater than T_{cure}. This suggests that the final T_g of an isothermally cured material is T_{cure}. In practice, the T_g usually appears higher than the cure temperature. This increase can occur for several reasons. First, even though the kinetics of the cure reactions are frozen by vitrification, diffusion controlled reactions can still occur. The material may cure more in the glassy state, and therefore exhibit a higher T_g overall. Another reason is the reaction enthalpy. When thermosetting materials cure via exothermic reactions, the temperature of the material is raised above the set isothermal cure temperature. In some cases (e.g. epoxies, polyamides, and cyanate esters) the reported T_g becomes 30-50°C higher than the isothermal cure temperature[A6-A7].

De-vitrification occurs when the T_g of a polymer decreases to the isothermal temperature, as in degradation. At high cure temperatures, other chemical reactions may occur, resulting in degradation. This degradation marks the lifetime of a material's performance under certain conditions. In the special case of materials with a high T_g, cure and thermal degradation reactions may compete with each other and result in a change in T_g[A2].

When examining two phase systems, phase separation may occur due to a developing immiscibility of the components[A2]. Usually materials begin their cure as homogeneous solutions, but as the cure proceeds and the homogeneous composition balance is altered, the materials form multi-phase-separated morphologies. The cure of two phase systems often involves at least two sequences; a controlled morphology must be developed by gelling the material at one temperature, and a post-cure is needed to complete the chemical reactions.

Several methods have been developed to observe the events that occur during cure of thermoset materials. The times to gelation and vitrification can be seen by a combination of techniques including torsional braid analysis (TBA) and melt rheology[A8]. These times are also reported on the basis of dynamic mechanical spectroscopic methods. Analysis of the change in dynamic mechanical properties of reactive systems reveals that the gel point can be obtained when tan δ (G''/G') or the loss modulus (G'') pass through a maximum as observed in Figure A2[A1,A8].

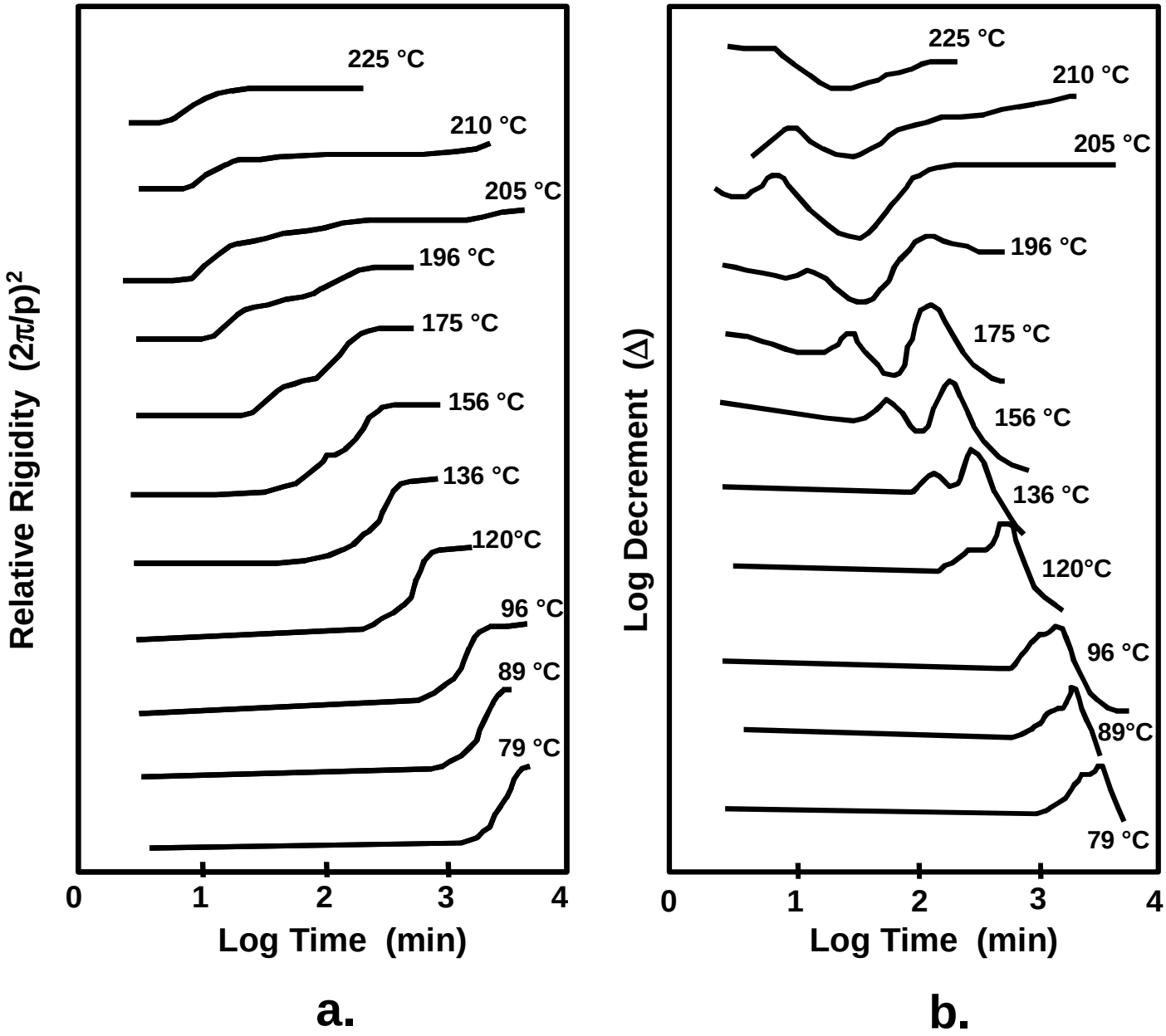

Figure A2. Isothermal Torsional Braid Analysis Spectra(A8)
a) Relative Rigidity
b) Log Decrement

Some authors suggested that the gel point could be obtained from the intersection of the loss and storage modulus (G')[A9]. This would be determined when tan $\delta = 1$, since tan $\delta = G''/G'$. However, theoretical calculations revealed that the intersection of the loss and storage modulii satisfies the gelation criteria only for a certain law of relaxation behavior of the material and the coincidence of the intersection at the gel point is an exception[A10].

Other techniques have also been used to develop these diagrams. Variations in Rayleigh-Brillouin scattering during cure of an epoxy were compared to torsional braid analysis (TBA) results of the same material[A15]. This work suggested that the scattering technique was more sensitive to gelation measurements than TBA because scattering intensities increased drastically during fluctuations in material density. The authors related the density fluctuations to gelation, and suggested that low frequency measurements were insensitive to these fluctuations.

Many thermosetting materials have been examined during cure, and their TTT diagrams developed. Among these are epoxies, polyamides, phenolic resins, and bismaleimides. The most common materials studied are epoxy resins[A11-A14]. By changing the curing agents and stoichiometry of the epoxy reactants, the cure kinetics were altered. This also produced different times to the curing events (physical properties). A correlation was then drawn as to the effect each reactant variance had on each of the physical events of the cure.

A.1.2 Effects of Toughening on Thermosetting Materials

The modification of a brittle material by the addition of another, more energy absorbent material has been employed extensively to "toughen" a number of polymeric systems. Thermoset materials, which are inherently brittle due to their highly crosslinked structure, have been modified by a variety of polymers to increase material toughness. The more popular of these tougheners are high temperature thermoplastics[A17-A20] and rubbers[A16]. The high temperature thermoplastics achieved moderate levels of toughness without sacrificing the high temperature performance properties of the thermosetting materials. Kinloch [A16] in a review on rubber toughened polymers listed some of the factors believed to contribute to the toughness of a rubber-modified epoxy. These factors included cross-link density and T_g of the matrix, rubber phase volume fraction, particle size, size distribution, morphology, and the interphase region between particles and matrix. Recent efforts have shown that these factors hold true for thermoplastic toughened epoxies as well[A19-A23].

Phase diagrams are important in explaining the phase separation process in polymers. Figure A3 is a phase diagram in terms of temperature, molecular weight, interaction parameter (χ), and volume fraction. Displayed is a material characterized by an upper critical solution temperature or UCST. Above this critical temperature, the blend exists as a one-phase mixture. Sudden cooling or quenching the blended material will cause one of three events to occur. If the

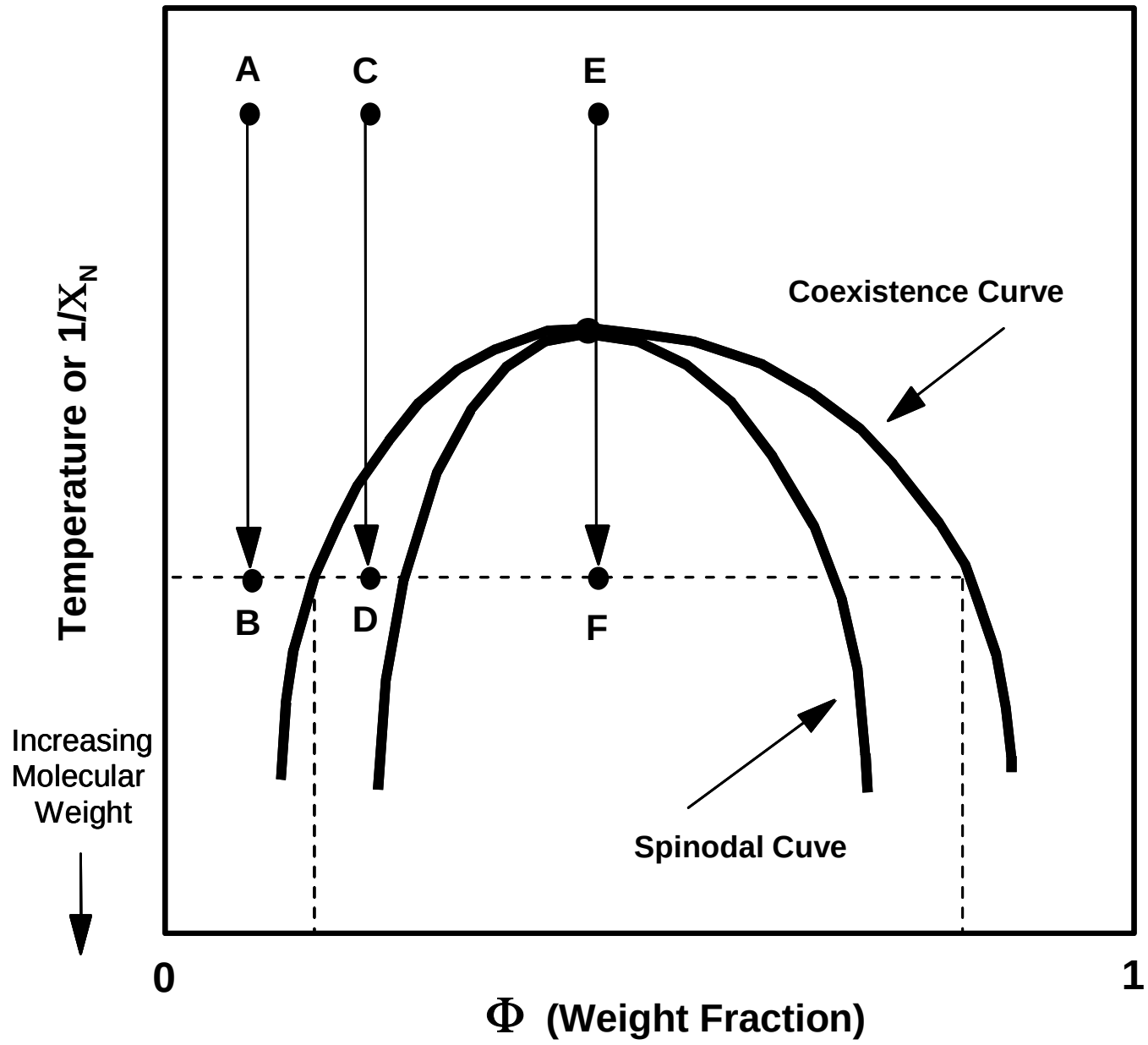

Figure A3. **Phase diagrams in terms of temperature, number of repeat units, and interaction parameter.[A24]**

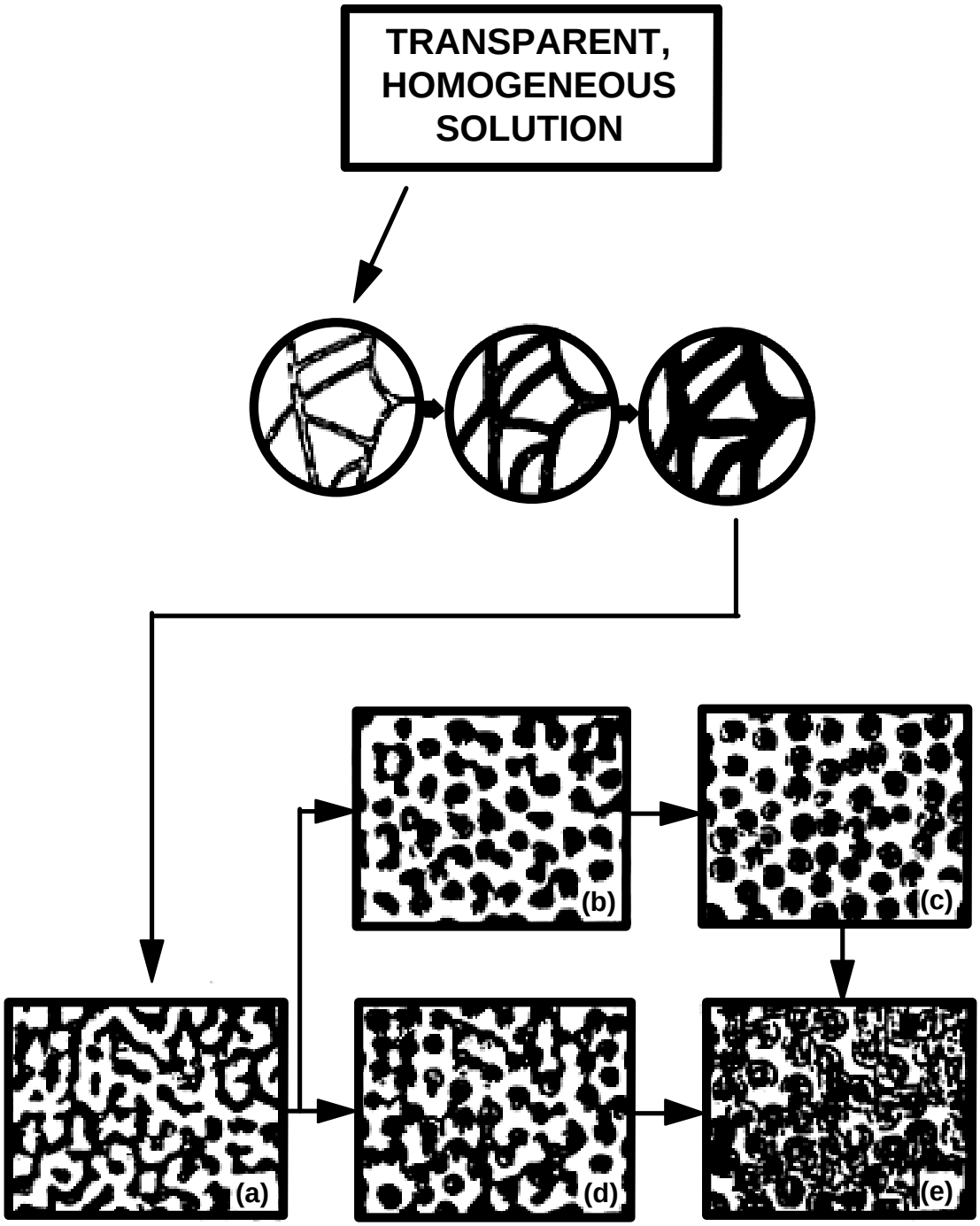

Figure A4. Morphologies resulting from spinodal decomposition.[A25]

a.) Co-continuous phase morphology
b.) Beginning stages of micro-phase formation, white phase dominant
c.) Micro-phase structure, white phase is continuous
d.) Beginning stages of micro-phase formation, black phase dominant
e.) Micro-phase structure, black phase is continuous

blend is quenched from point A to point B, the material will remain a one-phase system. Quenching from C to D will result in a binodal phase separation. The area between the coexistence curve and the spinodal curve is the metastable region. In this region, an energy barrier to nucleation exists. Once this barrier is overcome, a large number of particles precipitate from the blend and grow larger with time. Spherical particles are usually the end result of phase separation in this manner. If the blend is quenched from E to F, phase separation occurs through spinodal decomposition. The area under the spinodal curve in Figure A3 represents an unstable region, whereby, phase separation is continuous and spontaneous[(A24)].

It is usually a rapid process with favorable thermodynamics. Figure A4 is a schematic characterization of spinodal decomposition[(A25)]. As spinodal decomposition begins, initial fluctuations in concentration occur, precipitate, and grow until two phases are produced. Immediate precipitation results in an interlocked structure that continues to thicken until globules are formed due to surface tension effects. These globules are described as being similar to the spherical particles in binodal decomposition. Molecular weight changes during phase separation are also displayed in Figure A3[(A26)]. If molecular weight replaces temperature on the y-axis with higher molecular weights near the origin, then quenching the two-phase system from A to B (increasing molecular weight) still results in a one-phase system. Quenching from C to D results in a metastable material and from E to F results in an unstable material where phase separation occurs by spinodal decomposition. Changes in molecular weight and

interaction parameter may readily occur as a result of processing reactive blends, and therefore the phase separation process needs to be well characterized for processing compatibility.

A.2 EXPERIMENTAL METHODS AND TEST PROCEDURES

The cyanate ester thermosetting material used in this investigation was prepared in a manner similar to that described in Chapter 3. The monomer was heated at 100°C until melted, degassed, and the co-catalyst mixture was added. In the cases where toughened materials were required, 25% of the phenolphthalein-based poly(arylene ether sulphone) was added to the monomer prior to the degassing stage of preparation. The blended material was allowed to cool down to its crystalline form until use. Preparation of the sample for the curing experiments consisted of re-heating to 100°C until completely melted, stirring at 100°C to re-disperse the catalyst and thermoplastic toughener evenly throughout the mixture, and then coating the material onto a support medium prior to the measurement.

A Polymer Laboratories Dynamic Mechanical Thermal Analyzer (DMTA), Mark II model, in both bending and shear mode was utilized for the observation of the cyanate ester cure behavior. The instrument has the capability of scanning through several frequencies during an experiment. A frequency of 1 Hz was arbitrarily chosen as the standard applied frequency. When multiple frequency experiments were performed, three frequencies were scanned using 1 Hz as the

midpoint and moving out one decade on either side as the other two frequencies (0.1Hz, 1Hz, 10Hz). Tests were performed over a range of isothermal temperatures for times as high as 400 minutes. In most cases, the experiment was stopped immediately after "the vitrification peak" was observed. The first attempt to examine the cure of these materials was performed in a bending mode setup (Figure A5a). A 1-inch X 0.5-inch titanium wire mesh was plasma treated in an oxygen atmosphere for one minute to enhance surface wettability. The uncured cyanate ester material (untoughened or toughened) was then heated to 100°C and upon melting was coated onto the mesh for testing. The sample was then cooled and clamped into the instrument in a single cantilever fashion and torqued to 40 N/cm^2. For analysis, small knife-edge clamps were used with a small sized instrument frame.

A second attempt to measure cure properties utilized the shear mode clamps of the instrument (Figure A5b). Uncured cyanate ester material was coated onto the shear studs to approximately 0.1mm thickness. These studs were then placed into the instrument and, with a hot air gun to melt the material, adjusted to the proper tension. This tension was estimated by slowly tightening the probe until a tan δ reading on the instrument LCD panel registered a consistent number. Proper tension was also judged by instrument behavior. If the studs were too close to the center block, a "stuttering movement" was observed in the driveshaft vibration. The studs being too far from the block displayed a highly scattered noise in the tan δ readout. Once proper tension was established, the

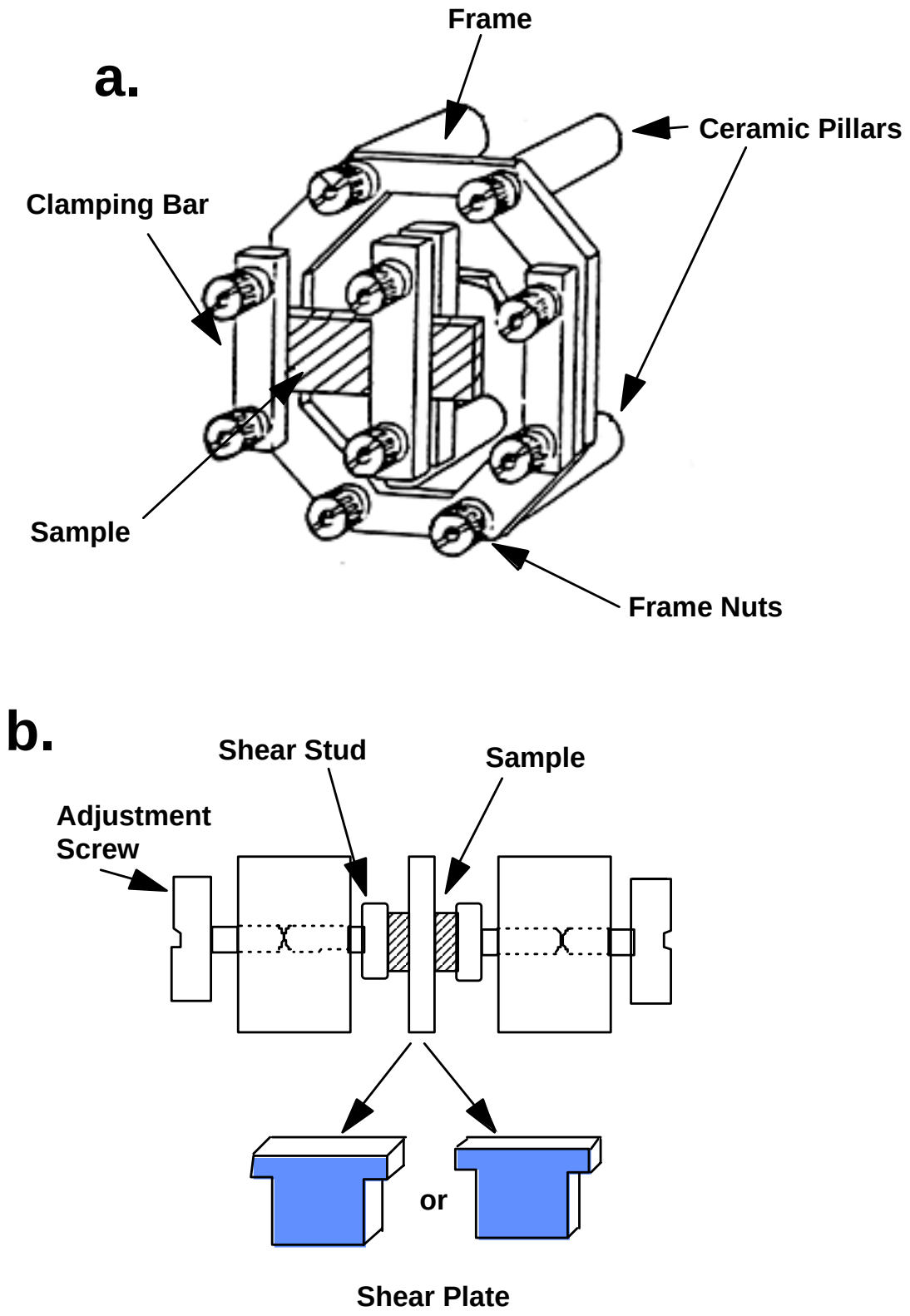

Figure A5. a) Single cantilever bending mode sample arrangement
b) Shear sandwich arrangement

oven was mounted, ramped to temperature at 10°C/min., and data collection initiated. This method was more accommodating with the 25% toughened samples due to the higher initial viscosity from the incorporation of the thermoplastic. The third attempt reverted back to bending mode operation. The material and instrument were setup in the same manner as above with two notable exceptions. Before sample mounting, the frame and clamps were treated with a Teflon mold release agent and doubly coated with aluminum foil. Also, the threads of the mounting screws were coated with an anti-seize agent. These protective measures were taken to assure that the instrument head would not be "glued" together after the thermoset cure. This last approach proved the most reproducible and was still relatively easy to perform. Experimental data were collected and exported to a Macintosh graphing program for interpretation and analysis.

A.3 RESULTS AND DISCUSSION

A.3.1 Initial Bending Mode Experiment

The first attempt to characterize the cure properties of cyanate esters was done by using the DMTA in the bending mode. Figure A6 shows the data obtained from that experiment. Displayed is the storage modulus, E',
and tan δ (E''/E') vs. cure time at 150°C isothermal cure temperature for the neat cyanate ester resin. The data strongly support the use of forced oscillation

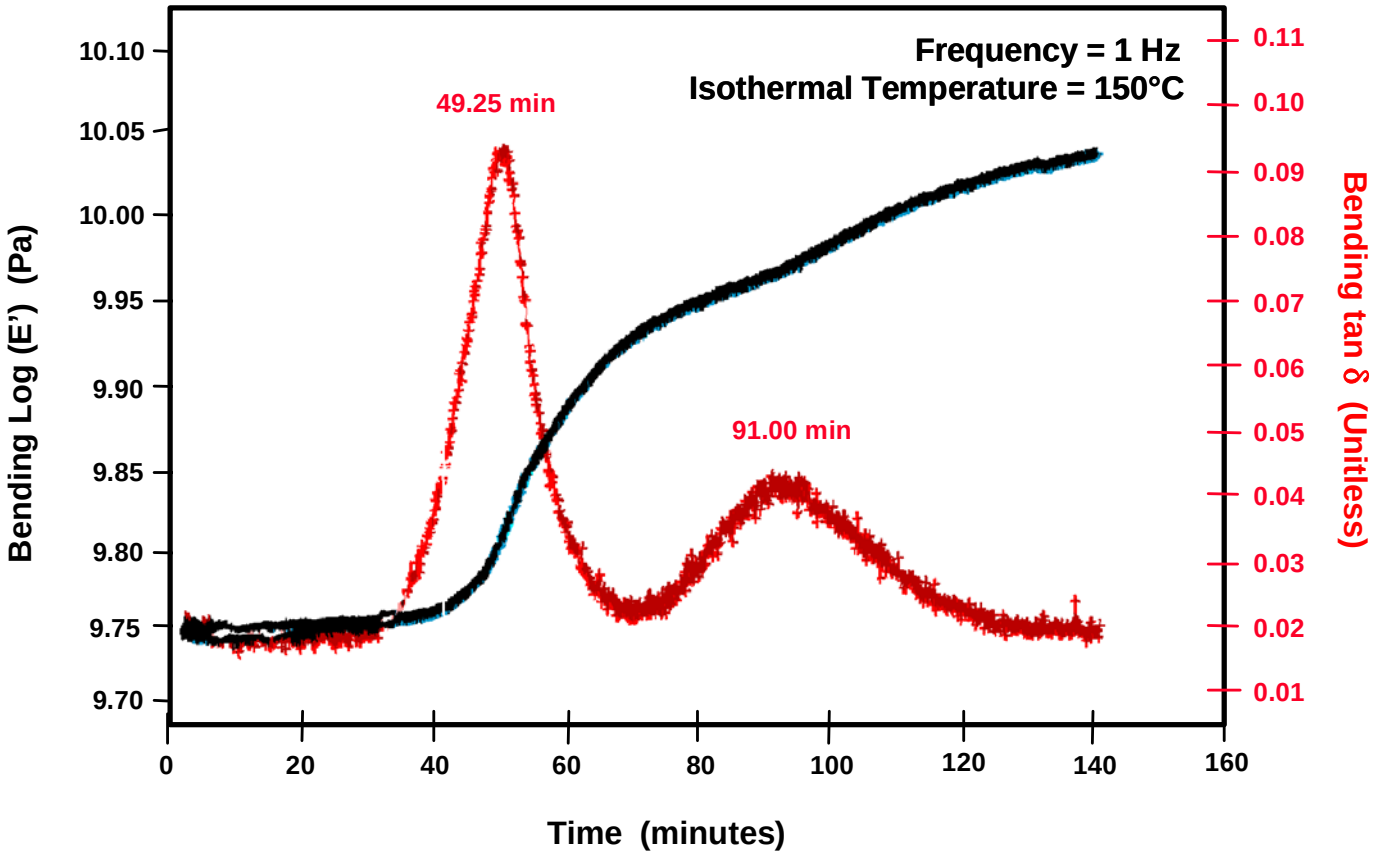

Figure A6. 150°C isothermal DMA measurement in bending mode of the cure of neat Cyanate ester resin. Data was collected at an applied frequency of 1 Hz.

experiments as a viable alternative to torsional braid analysis in developing TTT diagrams. Two distinct peaks in tan δ were observed, occurring at 49 minutes and 91 minutes, respectively. They were attributed to gelation and vitrification of the material at the applied frequency of the test, in this case 1Hz. The storage modulus (E') correlated well with the tan δ, increasing dramatically at the same times as the tan δ was maximizing. This correlation supports the occurrence of gelation and vitrification during cure, respectively.

As a confirmation of the gel point, Srinivasan[A27] examined the isotherrmal melt viscosity during cure. Figure A7 illustrates that data and displays the information obtained for both the unmodified cyanate ester and the 25% toughened material. The toughener employed was identical to that employed in this research. Since gelation is defined as the formation of an infinite network, the viscosity at the gel point approaches infinity. Table A1 displays the estimated times, in minutes, to infinite viscosity. Interesting results are observed, and do not appear to agree with the dynamic results. The times to gelation in the viscosity measurements are considerably larger than in the DMTA experiment. However, the time required to reach the cure temperature in the DMTA experiment must also be considered in the time to gelation. The temperature ramping in DMTA causes some cure to take place before data acquisition begins. As long as each sample sees the same thermal treatment, however, the trends in the data should be proportional. The second peak is assigned to vitrification of the material, since after this point in the cure, the material was glassy in appearance.

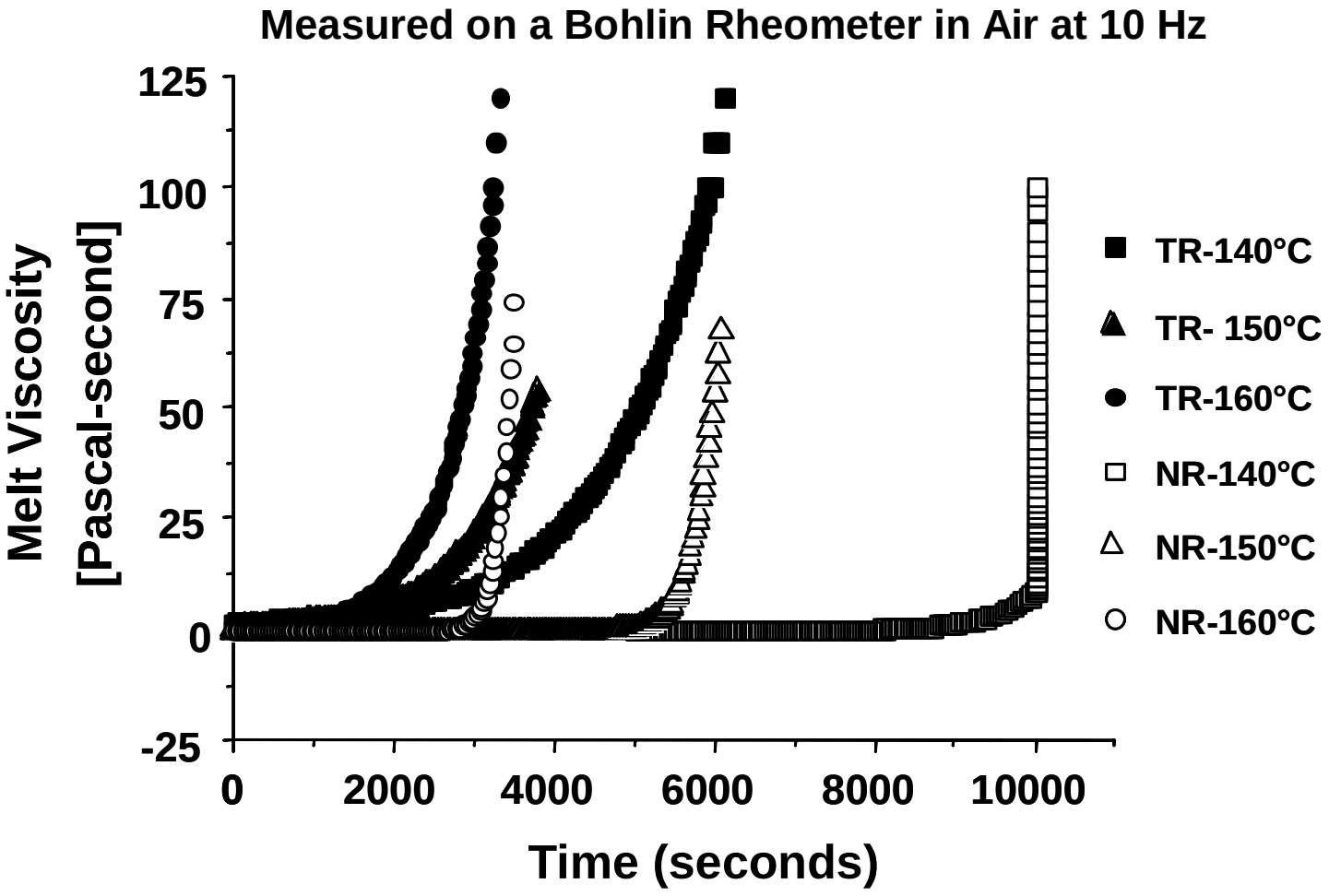

NR: Neat Resin;
TR: 25% 15K PPH-PSF-OH Thermoplastic Toughened Resin

Figure A7. Isothermal melt viscosity (Pa*s) as a function of time (min) of the neat resin (NR) and the 25% toughened resin (TR).[(A27)]

Isothermal Cure Temperature °C	Unmodified Cyanate Ester Resin (NR)	25% Modified Cyanate Ester Resin (TR)
140 °C	167 min.	103 min.
150 °C	103 min.	67 min.
160 °C	58 min.	56 min.

Table A1. Gel point determination from isothermal melt viscosity data.[A27]

Unfortunately, the low viscosity of the cyanate monomer at the isothermal cure temperature resulted in uncured material flowing into the frame mounts of the instrument. Once the second peak was observed (vitrification reached), the clamps and frame of the instrument were permanently cemented to the rest of the instrument. Besides confirming that vitrification was obtained, replacement of the instrument head after each experiment was not a viable option. This led to the development of a different method for obtaining the cure data.

A.3.2 Shear Mode Experiments

Shear mode DMTA, is a very sensitive technique, and a viable alternative to the difficulties observed in the bending mode experiment. The experimental setup consisted of an aluminum block mounted to the drive shaft of the instrument, and two circular aluminum studs mounted to the frame. This arrangement insured that the shear mode alternative was preferred due to the disposability of the probes after the experiment was finished. Unfortunately, the data obtained suggest many other obstacles are involved when using this technique.

Figure A8 displays a set of isothermal curves developed using the instrument in the shear mode. Represented are the neat cyanate ester isothermal cure curves at 150, 160, 170, and 180°C, respectively. The first observation about this data

A-8a.)

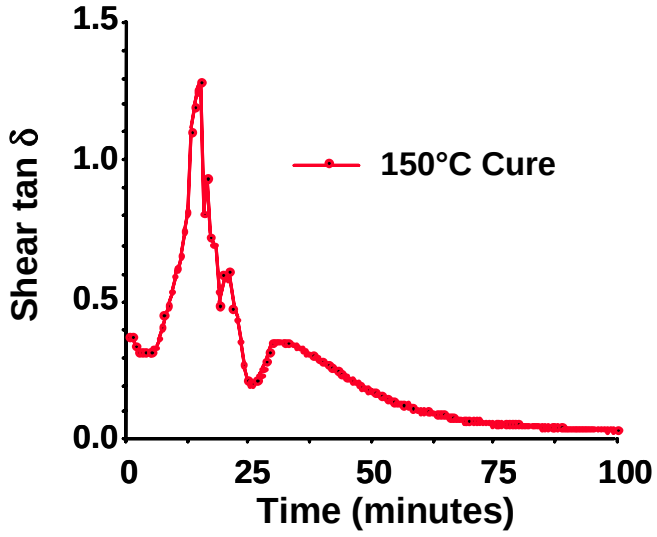

A-8b.)

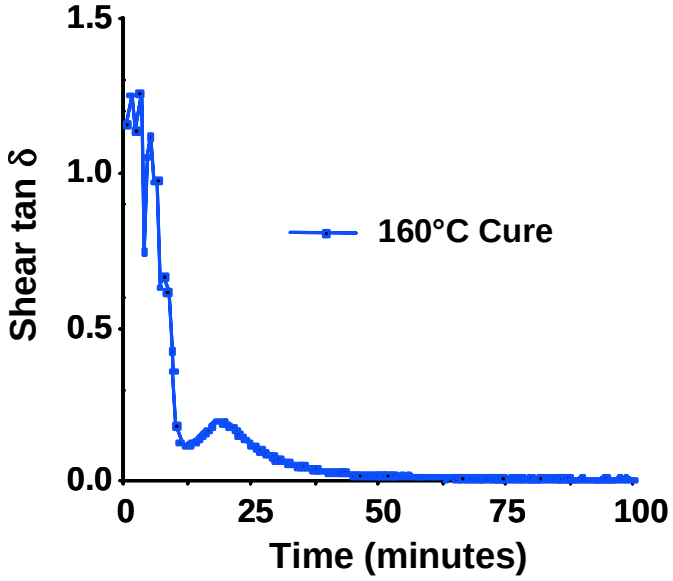

A-8c.)

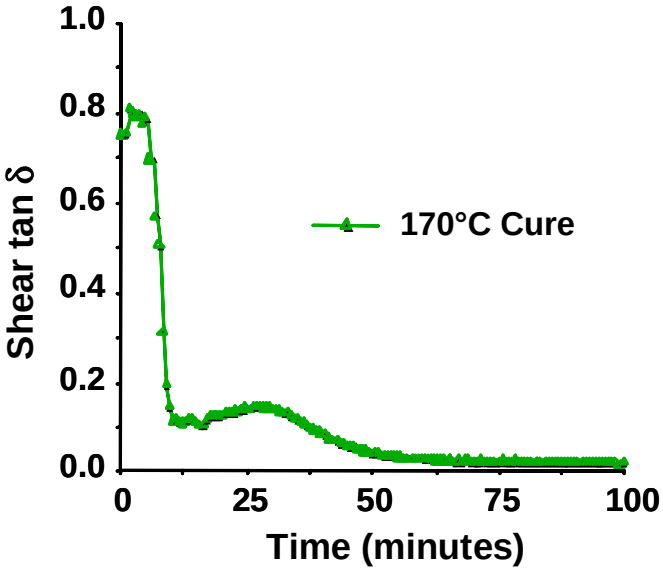

A-8d.)

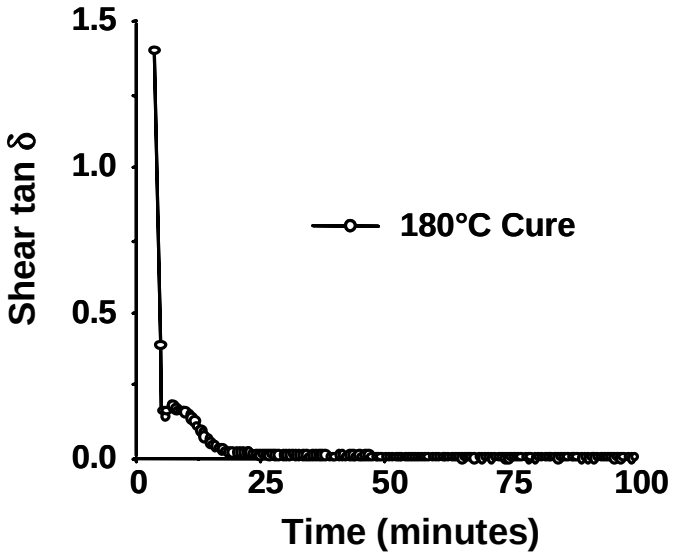

Figure A8. Comparison of isothermal cure temperature on the cure properties of Cyanate esters. Shear mode DMTA.

a.) 150°C Cure
b.) 160°C Cure
c.) 170°C Cure
d.) 180°C Cure

is that the resolution of the peaks is greatly diminished when compared to the bending mode experiment. This diminished resolution was strongly influenced by the method and subsequent placement of the sample. Satisfactory technique required delicate placement of the test sample between the studs and center block of the shear apparatus. Upon heating, the viscosity decrease unfortunately allowed the material to flow from the studs. Another concern was proper data acquisition. The studs required a horizontal and equal displacement from the center plate. Also, the decreased amount of material used to examine the cure process in this thesis, and the lack of a support medium to reduce flow at higher temperatures complicated the experimental technique. Any one, or all, of these problems occurring during the experiment resulted in a loss of resolution and reproducibility of the data. Since the viscosity of the pure monomer at elevated temperatures plays a hindering role in obtaining the isothermal cure data; the 25% thermoplastic modified material was used. This material displayed a higher initial viscosity, and less initial flow would result at the beginning of the cure run.

The set of curves in Figure A9 represents the isothermal cure data obtained from shear mode DMTA, when the 25% thermoplastic toughened monomer was employed. Data resolution was increased some, but difficulty still remained in assigning peaks to physical changes occurring during the cure. It appears from these representative curves that peaks can be associated with phase separation, gelation, and vitrification, respectively. However, with the large amount of scatter in the data and the inconsistency of where the peaks develop, the data must be

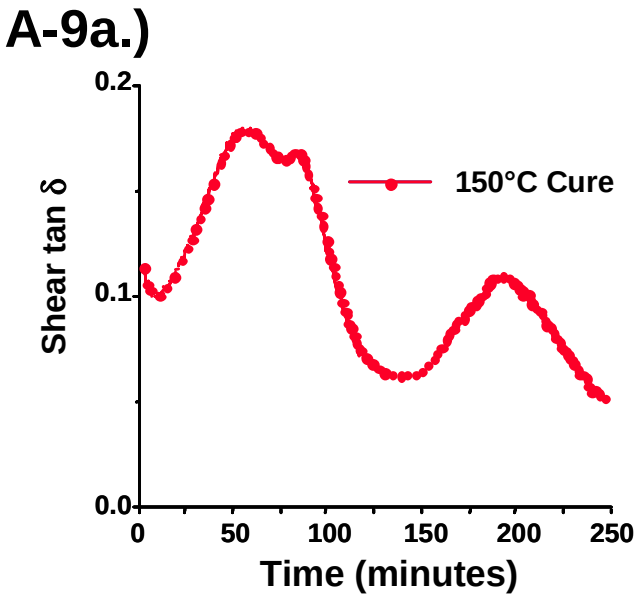

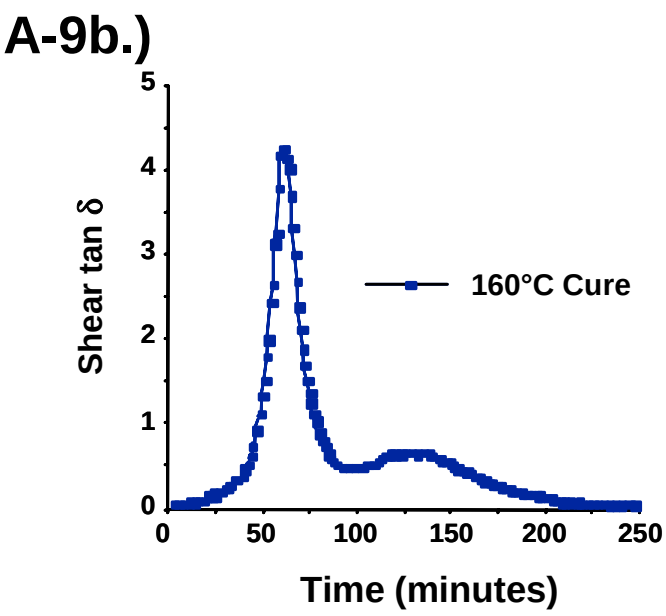

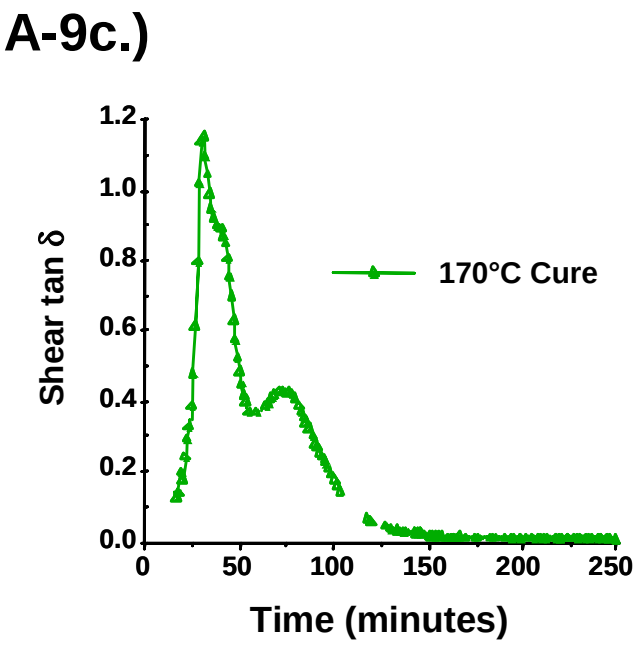

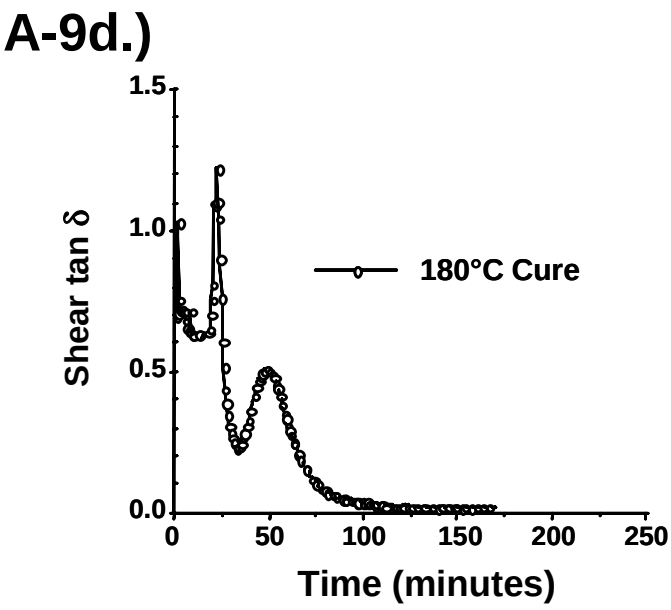

Figure A9. Comparison of isothermal cure temperature data for 25% toughened cyanate ester

a.) 150°C Cure
b.) 160°C Cure
c.) 170°C Cure
d.) 180°C Cure

considered tentative. Furthermore, reproducibility of the data was very difficult to obtain. This is represented in Figure A10, which displays four separate isothermal experiments performed at 160°C. The first curve is that also depicted in Figure A9. The others represent additional attempts to repeat this first set of data. The results show distinct peaks that shift at random with respect to time. This lack of reproducibility stems from the sensitivity of the technique and inherent problems as discussed above.

A.3.3 Experimental Alternatives

Clearly, the inconsistent scatter obtained from the shear mode DMTA experiments as well as the promising results obtained from the initial bending mode experiments, prompted the investigation of other methods to obtain the cure properties of cyanate ester resins. The first attempt utilized two glass slides as a support medium (glass/sample/glass sandwich) in the bending mode of the DMTA to develop the isothermal cure data. The thought behind this technique was that the surface forces created by putting the two slides together would keep the liquid from flowing upon heating. Also, the modulus of the glass was sufficiently high to provide proper support for reproducible information to be obtained without destruction of instrument parts. Unfortunately, this technique was not successful since the pressure was too great when clamping the slides into the instrument, and they kept breaking before the experiment began. Final experiments incorporated the original testing method of coating the uncured resin on a titanium mesh and collecting data in the bending mode.

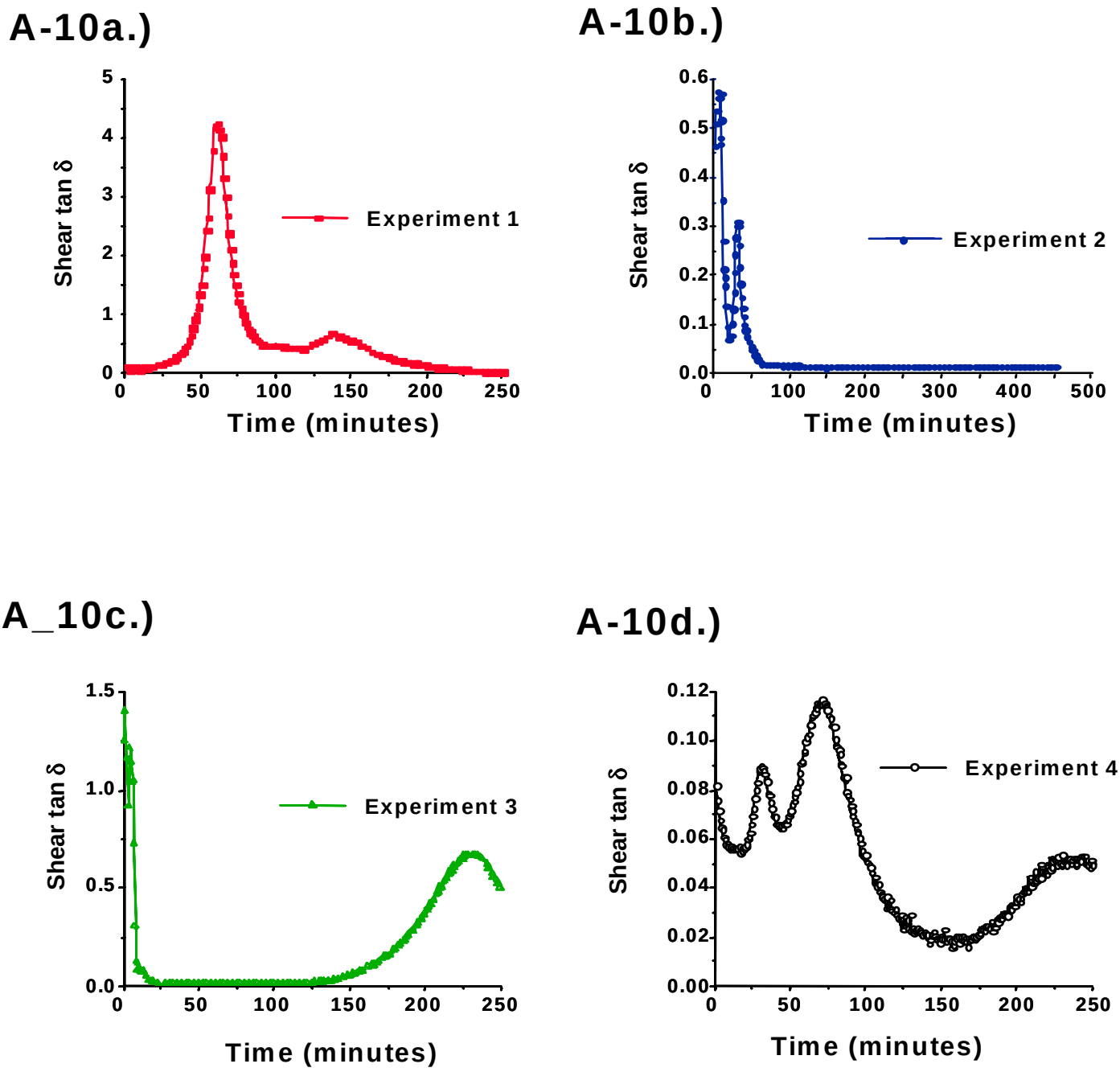

Figure A10. An attempt at reproducibility in shear mode experiments. Isothermal cure temperature was 160°C for all experiments.

a.) Experiment 1
b.) Experiment 2
c.) Experiment 3
d.) Experiment 4

Modifications were made to the original experiment by carefully wrapping the bending mode frame and the test clamps with aluminum foil and applying an anti-seizing agent on the frame support screws. This was done to keep the instrument parts from being bonded together. Initial results suggest this method was satisfactory for completion of this investigation.

Figure A11 shows the data obtained from the neat resin using the safeguarded bending mode setup described above. Two separate experiments were conducted at an isothermal cure temperature of 150°C. The data displayed is tan δ vs. cure time. Now one notes that the isothermal cure data is reproducible. Although some peak shifting on the time axis occurs, the variation is not nearly as apparent as that shown in Figure A10. The peak shifting is probably caused by the initial heating rate varying slightly between samples. This was shown to be controlled by immediate introduction of the material into an oven at the isothermal cure temperature. The important difference between this methodology and the other techniques is that similar peaks did occur in both experiments and are reproducible between experimental runs.

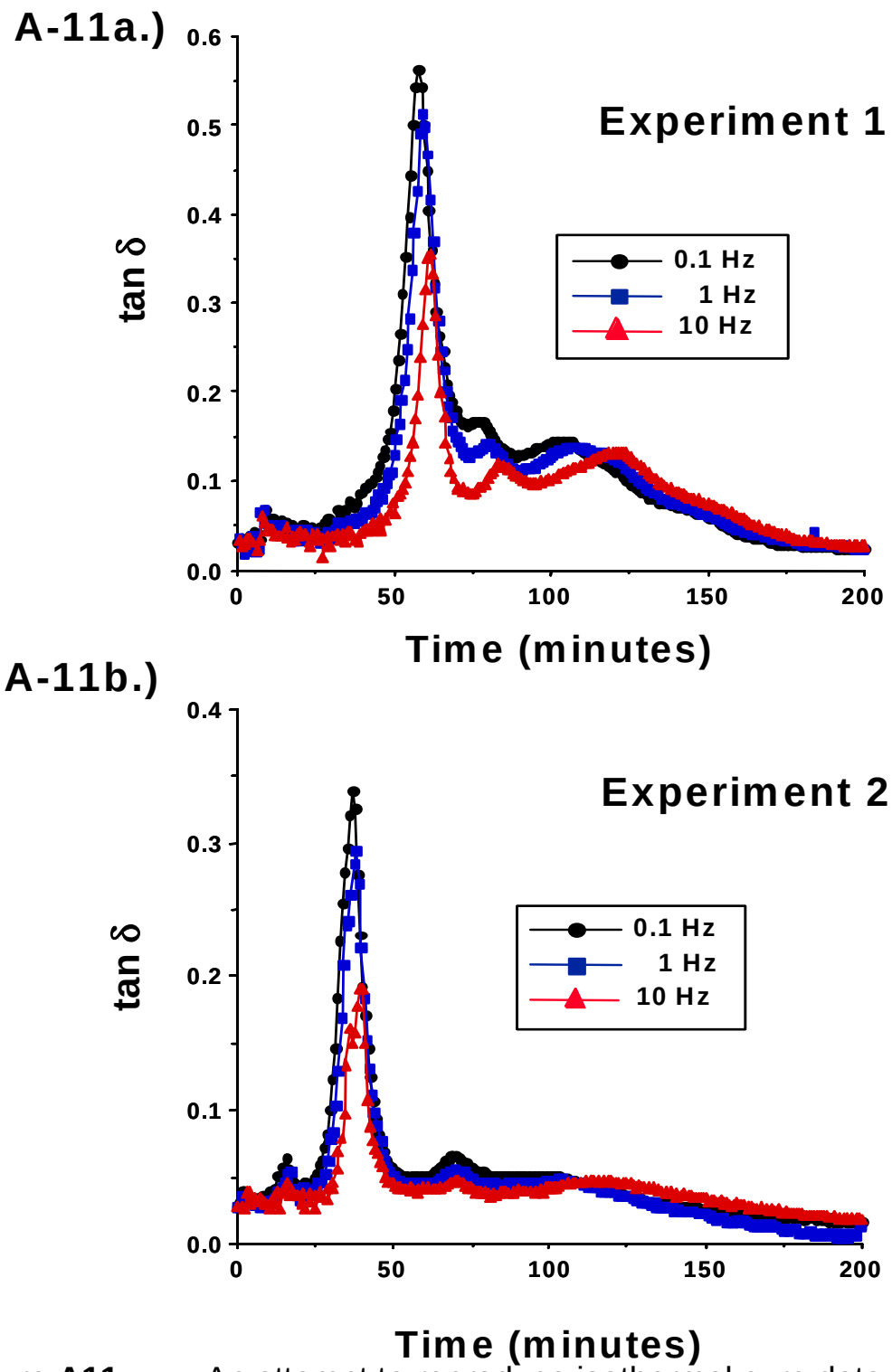

Figure A11. An attempt to reproduce isothermal cure data in the protected bending mode. Isothermal cure temperature was 150°C.
a.) Experiment 1
b.) Experiment 2

A.4 Summary

The cure of thermosetting materials is a rather complicated process that requires an understanding of the kinetics and physical changes that occur in the material during processing. However, developing a measurement technique to follow these changes during cure is also a complicated endeavor. Several attempts were made to study the transient physical properties of a cyanate ester material during thermosetting using dynamic mechanical analysis. Bending mode experiments were the most promising, being fast and easy to obtain the information sought. Unfortunately, the decrease in initial viscosity of the material at elevated cure temperatures resulted in permanently bonded instrument parts and it was necessary to identify another method. Subsequently, shear mode experiments were evaluated and showed promise. The involved instrument parts were disposable, but reproducibility and peak resolution were relatively non-existent. Finally, re-applying the bending mode procedure, with extensive flow protection, produced results that were more desirable.

A.5 REFERENCES

A1. J. K. Gillham, Polym. Eng. Sci., **19**, 676 (1979).

A2. J. K. Gillham, Polym. Eng. Sci., **26**, 1429 (1986).

A3. M. T. Aronhime, J. K. Gillham, Adv. Polym. Sci., **78**, 83 (1986).

A4. J. B. Enns, J. K. Gillham, J. Appl. Polym. Sci., **28**, 2567 (1983).

A5. P. G. Babayevsky, J. K. Gillham, J. Appl. Polym. Sci., **17**, 2067 (1973).

A6. J. B. Enns, J. K. Gillham, Adv. in Chem. Series, **203**, 27 (1983).

A7. L. C. Chan, H. N. Nae, J. K. Gillham, J. Appl. Polym. Sci., **29**, 3307 (1984).

A8. J. B. Enns, J. K. Gillham, J. Appl. Polym. Sci., **28**, 2831 (1983).

A9. H. H. Winter, F. Chambon, Polym. Bull., **13**, 499 (1985).

A10. H. H. Winter, Polym. Eng. Sci., **27**, 1698 (1987).

A11. P. A. Oyanguren, R. J. J. Williams, J. Appl. Polym. Sci., **47**, 1361 (1993).

A12. S. L. Simon, J. K. Gillham, J. Appl. Polym. Sci., **46**, 1245 (1992).

A13. S. L. Simon, J. K. Gillham, J. Coat. Technol., **65**, 57 (1993).

A14. N. Biolley, T. Pascal, B. Sillion, Polymer, **35**, 558 (1994).

A15. S. Kondo, T. Igarashi, T. Nakamura, J. Appl. Polym. Sci., **26**, 2337 (1981).

A16. *Rubber-Toughened Plastics*, C. K. Riew, ed., ACS Adv. in Chem. Series, **222**, 67 (1989)

A17. *"Toughening of Epoxy Resin Networks with Functionalized Engineering Thermoplastics",* ACS Adv. in Chem. Series, **233**, 293 (1993).

A18. S. P. Wilkinson, S. C. Liptak, J. J. Lesko, D. A. Dillard, J. Morton, J. E. McGrath, T. C. Ward, *"Toughened Bismaleimides and TheirCarbon Fiber Composites for Fiber Matrix Interphase Studies",* Proc. Sixth Japan-US Conf. Comp. Mat., 240 (1992).

A19. S. A. Srinivasan, J. E. McGrath, High Perform. Polym., **5**, 259 (1993).

A20. Radiation Effects on Polymers, R. L. Clough and S. W. Shalaby, eds., ACS, Washinton, D.C., 364 (1991).

A21. K. Yamanaka, T. Inoue, Polymer, **30**, 662 (1989).

A22. J. L. Hedrick, Ph.D. Dissertation, Virginia Tech, 1985.

A23. S. C. Liptak, Ph.D. Dissertation, Virginia Tech, 1993.

A24. A. J. Ryan, Polymer, **31**, 707 (1990).

A25. K. Yamanaka, Y. Takagi, T. Inoue, Polymer, **30**, 1839 (1989).

A26. S. M. Moschiar, C. C. Riccardi, R. J. J. Williams, D. Verchere, H. Sautereau, J. P. Pascault, J. Appl. Polym. Sci., 42, 717 (1991).

A27. S. A. Srinivasan, Ph.D. Dissertation, Virginia Tech, 1994.

APPENDIX B: DEVELOPMENT OF MEASUREMENT METHODS FOR CURE PROPERTIES USING REMOTE SENSING DIELECTRIC THERMAL ANALYSIS

B.1 Literature Review

B.1.1 Introduction

In recent years, considerable efforts have been made to monitor the cure process of thermoset materials in real time. As part of these efforts, various cure-sensing methods have been proposed, of which dielectric analysis appears to be quite promising. This technique consists of three major steps[(B-1)]:

- Measurement of a signal related to some dielectric property of the thermoset,
- Conversion of the measured signal to the appropriate value of the dielectric response
- Conversion of the experimentally determined dielectric property to cure properties of the material.

Of these steps, the first two are well developed; the technology is available to sense the appropriate signals, and models exist for conversion of these signals to dielectric properties[(B-2 - B-13)]. Most problems arise from attempting to convert the dielectric properties to cure details associated with a time-temperature-transformation (TTT) diagram. This review explains the theory developed to

satisfy the above steps, and discusses some of the advancements made for developing a TTT diagram from these measurements.

B.1.2 Remote Sensor Dielectric Analysis

Dielectric remote sensors based on interdigitating gold electrodes (Figure B-1) are available for *in situ* monitoring. This technology has been used to follow cure[(B-13 - B-16)], phase separation[(B-18 - B-19)], diffusion[(B-17)], and changes due to aging. The basis of dielectric cure monitoring is explained in detail in references B-13, B-17, B-20, and B-21, however the following generally describes the process. Dipoles present in an un-cured resin orient to follow an applied, alternating electric field, and ions present in the material migrate toward the electrodes as permitted by viscosity, forming charged layers. As the cure is initiated and propagates, the viscosity of the material increases, which decreases the response of both the dipoles and ions. If the relaxation times of the electrically responsive molecules become longer than the time needed for the electric field to change polarity, the electrical response of the molecule will fall behind that of the field. Higher field frequencies cycle the polarity faster causing the response lag to occur earlier. The result is a progressively slower response to the field with increasing field frequency.

In a dielectric measurement, an applied alternating voltage is often designed to vary in a sinusoidal manner as displayed in Figure B-2. The response to this

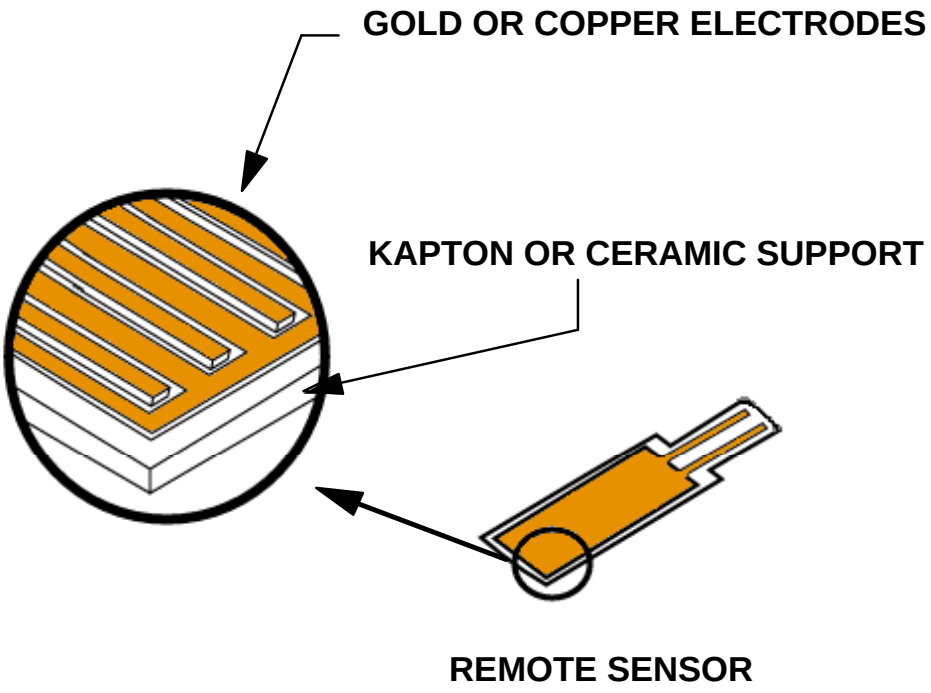

Figure B-1. Schematic representation of a dielectric remote sensor.[B-14]

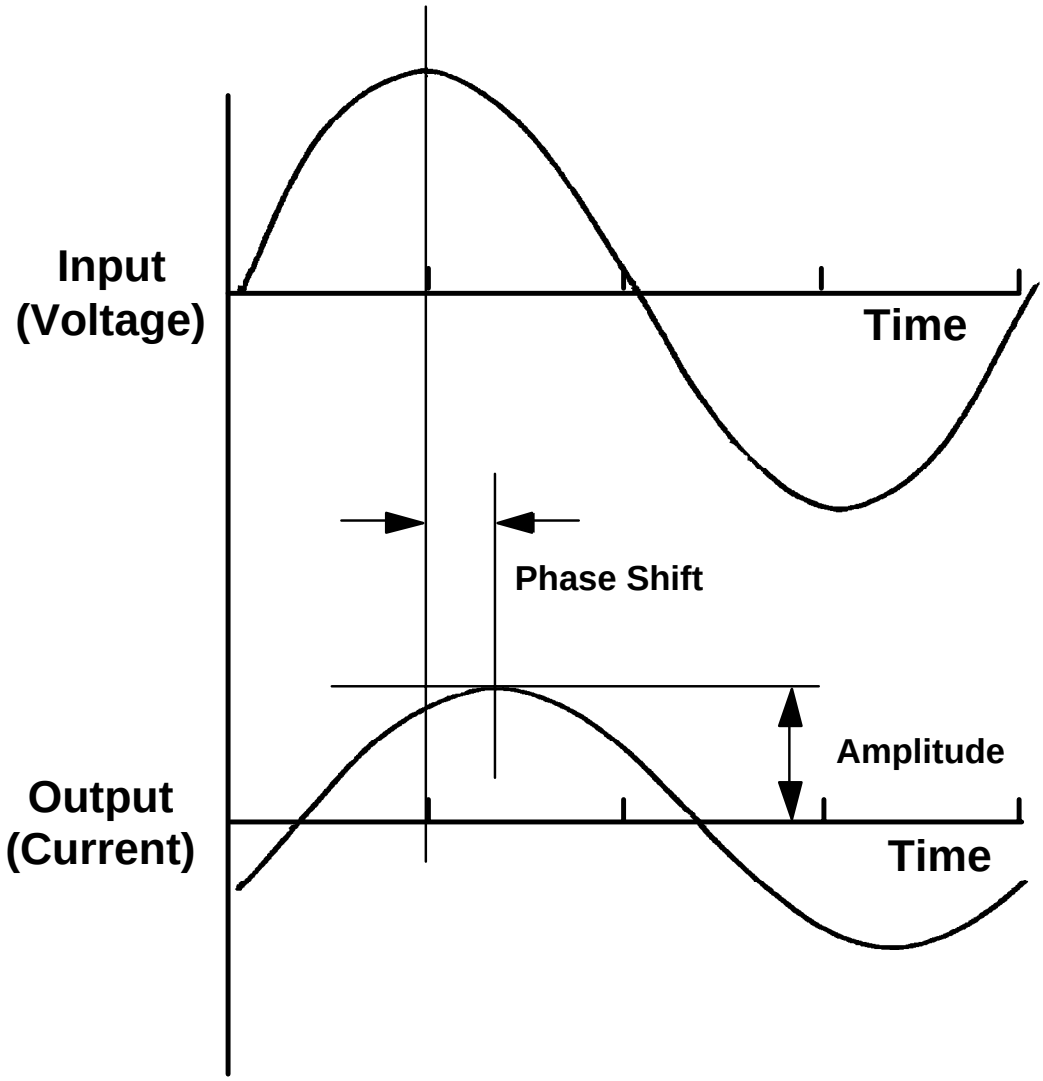

Figure B-2. Representation of applied voltage and current response.[B-24]

voltage (current) is also sinusoidal but differing in phase. These phase differences vary depending on the dielectric responsive material being studied and the temperature of the specimen. Frequency dependent measurements of dielectric impedance are characterized by the capacitance, C, and conductance, G, of a test sample and are used to calculate the complex permittivity,

$$\varepsilon^*(\omega) = \varepsilon'(\omega) - i\varepsilon''(\omega) \qquad \text{(B-1)}$$

where $\omega = 2\pi f$, f is the measurement frequency and C_0 is the air replacement capacitance of the sensor. The components of this complex permittivity are:

$$\varepsilon'(\omega) = \frac{C(\omega)\ \text{material}}{C_0} \qquad \text{(B-2a)}$$

and,

$$\varepsilon''(\omega) = \frac{G(\omega)\ \text{material}}{\omega C_0}\ . \qquad \text{(B-2b)}$$

These equations are accurate as long as the sensor's electrical properties remain constant throughout the experiment. Both the real ($\varepsilon'(\omega)$) and imaginary ($\varepsilon''(\omega)$) parts of the complex permittivity ($\varepsilon^*(\omega)$) can be composed of an ionic and dipolar component:

$$\varepsilon' = \varepsilon'_d + \varepsilon'_i \qquad \text{(B-3a)}$$

$$\varepsilon'' = \varepsilon''_d + \varepsilon''_i \qquad \text{(B-3b)}$$

The dipolar component, ε_d, arises from rotational diffusion of the molecular dipole moments or bound charge. The ionic component, ε_i, arises from the translational diffusion of charge. The dipolar term is usually dominant at high frequencies and in highly viscous media or samples. The ionic term dominates $\varepsilon^*(\omega)$ at low frequencies, low viscosity, and/or higher temperatures[B-23].

Ciriscoli *et al*[B-1] has recently critiqued dielectric cure measurement techniques. Attempts to quantitatively measure viscosity and degree of cure were discussed, and the two most widely accepted methods to determine these properties were examined. The two methods were proposed by Kranbuehl *et al*[B-8 - B-12], and Day and his co-workers[B-4 - B-7]. It was concluded that both methods were sensitive to similar ionic conductivities, resulting in the determination of the minimum viscosity of the sample and an indication of the end of the cure. Unfortunately, neither technique could determine the viscosity of the material during cure or the degree of cure, directly.

The methods used above evolved from testing homogeneous materials. Heterogeneous mixtures (i.e. modified thermosets) have also been examined([B-19, B-20, B-24], however, limited information exists on the effects of phase separation on dielectric cure data. Maistros *et al*[B-19] observed a significant effect on the dielectric behavior in a (reactive) rubber toughened epoxy, which was

proposed to be due to phase separation. They found a maximum in the storage permittivity, ε', at extremely low frequencies that corresponded to an increase in turbidity (measured by the power drop of an IR light source). This permittivity maximum was attributed to an interfacial polarization due to phase separation. The effect varied substantially with the applied experimental frequency, and was most pronounced at lower frequencies. High initial values of storage and loss permittivity were also observed due to electrode polarization at extremely low sample viscosity. After cure, electron micrographs revealed 0.5 micron diameter particles in the modified epoxy confirming phase separation had occurred.

Vitrification occurs in thermosets when the T_g of a material advances to the cure temperature. Researchers[B-14 - B-21] have suggested vitrification is observed as a dipole maximum in the dielectric loss factor or dielectric tan δ. This maximum was observed in a DGEBA epoxy system by Sheppard[B-21], and in a photocurable acrylate by Zumbrum[B-14]. A method of real time determination of T_g during cure was proposed by Day and Sheppard[B-17], who examined multi-frequency dielectric loss data of another DGEBA epoxy system. The ionic conductivity was related to T_g through the WLF relationship or a linear increase in log conductivity with T_g. MacKinnon *et al*[B-20] also made some interesting observations on the vitrification of these materials while studying the dielectric response to phase separation during cure. They employed a thermoplastic modified epoxy with relatively high amounts of thermoplastic toughener (20-30%). A maximum in the dielectric loss (**ε"**) curve and a slight increment in the storage permittivity for the unmodified

resin were attributed to vitrification. Increasing the amount of thermoplastic toughener decreased the resolution of the measurement. The dielectric information was modeled with peak shape as the only variable. Residual conductivity was observed to increase slightly with the addition of the toughener until a 20% ratio of thermoplastic to epoxy was obtained. Concentrations of toughener greater than 20% caused a decrease in conductivity. Vitrification appeared more clearly when the conductivity was mathematically removed from the model. This corresponds well with experimental observations since vitrification was detected well after phase separation of the material. The authors observed that the conductivity diminished throughout the cure and eventually reached an asymptotic value. From these observations, it was suggested the thermoplastic toughener acted as a diluent and delayed cure by increasing the gel time. The T_g of the cured modified epoxy was lower than that of the unmodified material, even though the T_g of the thermoplastic toughener was too close to that of the epoxy to be observed as a separate event. The above techniques have been sufficiently developed and were extensively employed in kinetic and cure studies of the cyanate ester thermosets discussed in Chapter 3 and Appendix A.

B.2 Experimental Methods and Test Procedures

The cyanate ester materials, both unmodified and modified with 25% poly(arylene ether sulphone), were prepared as described in Chapter 3 and Appendix A. Likewise, the same co-catalysts were added in the same manner, and the uncured material was cooled and then reheated prior to testing. A seven-day maximum shelf life for use was applied to assure no undesired curing before the experiment.

A Polymer Laboratories dielectric thermal analyzer (DETA) was utilized with the incorporation of a ceramic based remote dielectric sensor to follow the cure progression. Before use, the sensors were heated to 300°C and cooled at 0.1°C/min. to erase any thermal history they may have acquired during manufacture, and to avoid stress fracture of the sensor during the cure of the thermoset. Copper leads wrapped in heat resistant polyimide tape were then re-attached to the sensors using a conductive silver paint similar to that used by the manufacturer. This was done to avoid permanent attachment of the electrical leads to the sensor and to allow for more flexibility of the sensor in the oven. Small Teflon sensor mounts were attached to an aluminum plate with a commercial epoxy adhesive, and placed in a forced air oven at the desired isothermal curing temperature. The material was heated to 100°C to melt and coated on the sensors for testing while molten. Once data collection began, the

sample-coated sensors were placed into a forced air oven set to the isothermal curing temperature. Data was collected using a range of three frequencies and was then exported to a Macintosh graphing program for presentation and subsequent interpretation.

B.3 Results and Discussion

The basis of following the cure of thermosetting resins using dielectric remote sensors is explained extensively in references B-7, B-9, B-13, B-16, B-17, B-20 and in the preceding text. A dielectric remote sensor (schematic displayed in Figure B-1) consists of interdigitating gold or copper electrodes coated onto a ceramic or Kapton support. The electrodes act as capacitors and measure changes in amplitude and phase shifts of the current generated when there is an applied alternating voltage. From the collected information, storage dielectric (dielectric constant) and dielectric tan δ are obtained. Figure B-3 summarizes the information obtained form an isothermal cure experiment. Figure B-3a is the dielectric constant vs. cure time, and Figure B-3b is tan δ vs. cure time for the unmodified cyanate ester isothermally processed at 140°C. The experiment was performed at three frequencies, each varying by an order of magnitude. This was done to obtain a good representation of frequency dependence on the cure properties observed. The dielectric constant steadily decreases as cure proceeds, suggesting a steady decrease in ionic conductivity.

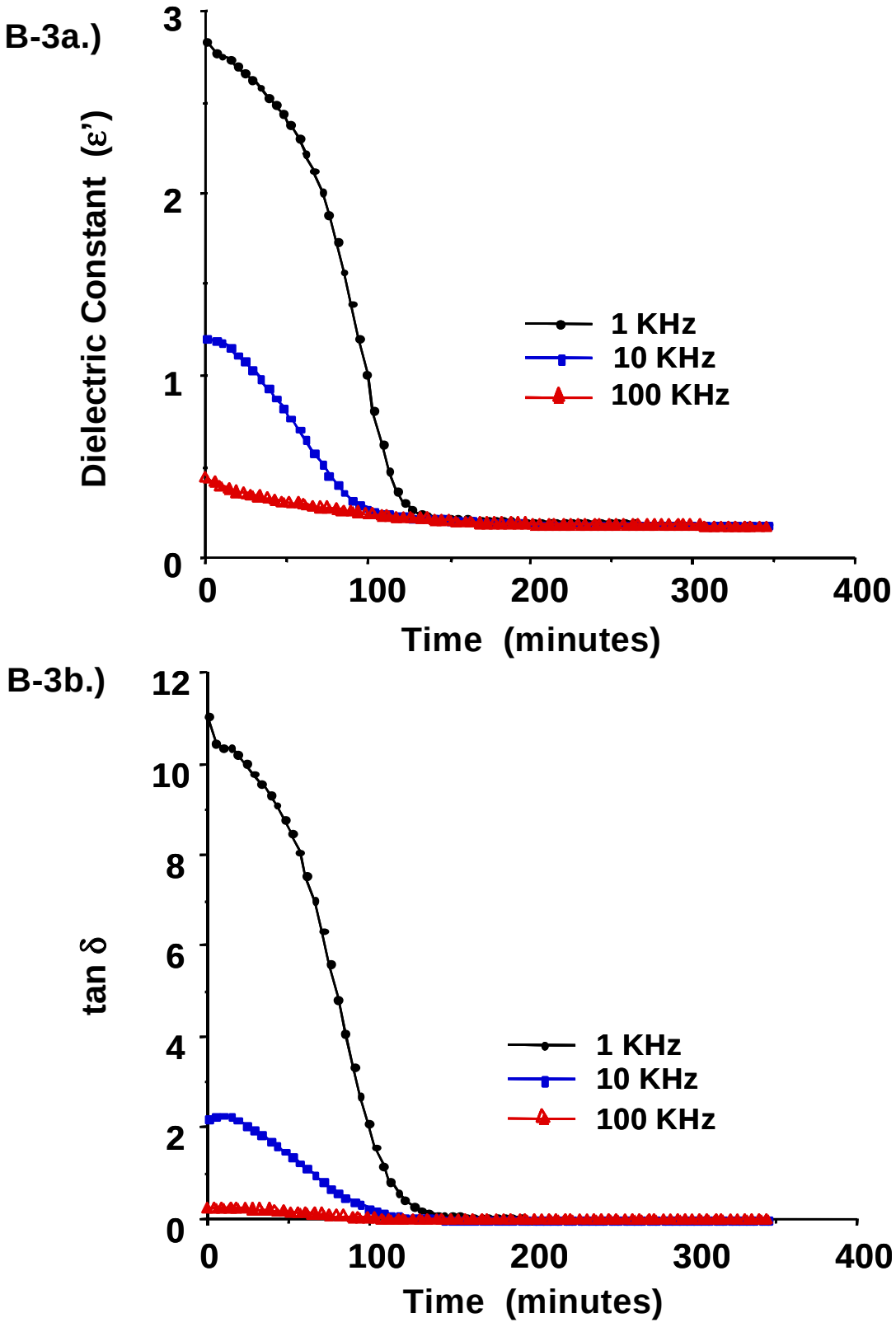

Figure B-3. Representation of Dielectric cure data for 140°C isothermally cured unmodified cyanate ester. Three frequencies were used to obtain the data.
a.) Dielectric Constant vs. Time
b.) Tan δ vs. Time

As previously discussed, this is related to an increase in viscosity of the thermoset as molecular weight increases. The tan δ response reveals much of the same information, and if inverted resembles an isothermal melt viscosity verses cure curve. A high ionic conductivity was present at the beginning of the reaction due to the low viscosity of the material at the cure temperature. This low viscosity allows for free movement of the ions present in the material and yields this high initial conductivity value. As the cure proceeds, the viscosity increases causing a more restricted flow of ions, and the ionic conductivity becomes less dominant. Once gelation is reached, ionic conductivity has little influence and the dipolar components of the storage and loss dielectric becomes the prominent response. The signal obtained due to dipolar alignment is significantly smaller in magnitude than for ionic conductivity and is therefore, masked on the plots due to the scale needed to display the ionic component. Expanding the dielectric constant and tan δ axes allows the dipolar component of the curves to be observed (Figure B-4). As a result of expanding the tan δ axis, a peak becomes visible around 160 minutes and occurs after the gel point suppression of ionic conductivity. As discussed earlier, dipolar alignment dominates at higher frequencies and in highly viscous media[(B-23)] due to the time scale of response and the lack of mobility of the ionic species. For this reason, the peak resulting from dipolar alignment is more evident in the 100 kHz measurement than in the two lower frequencies (Figure B-4b).

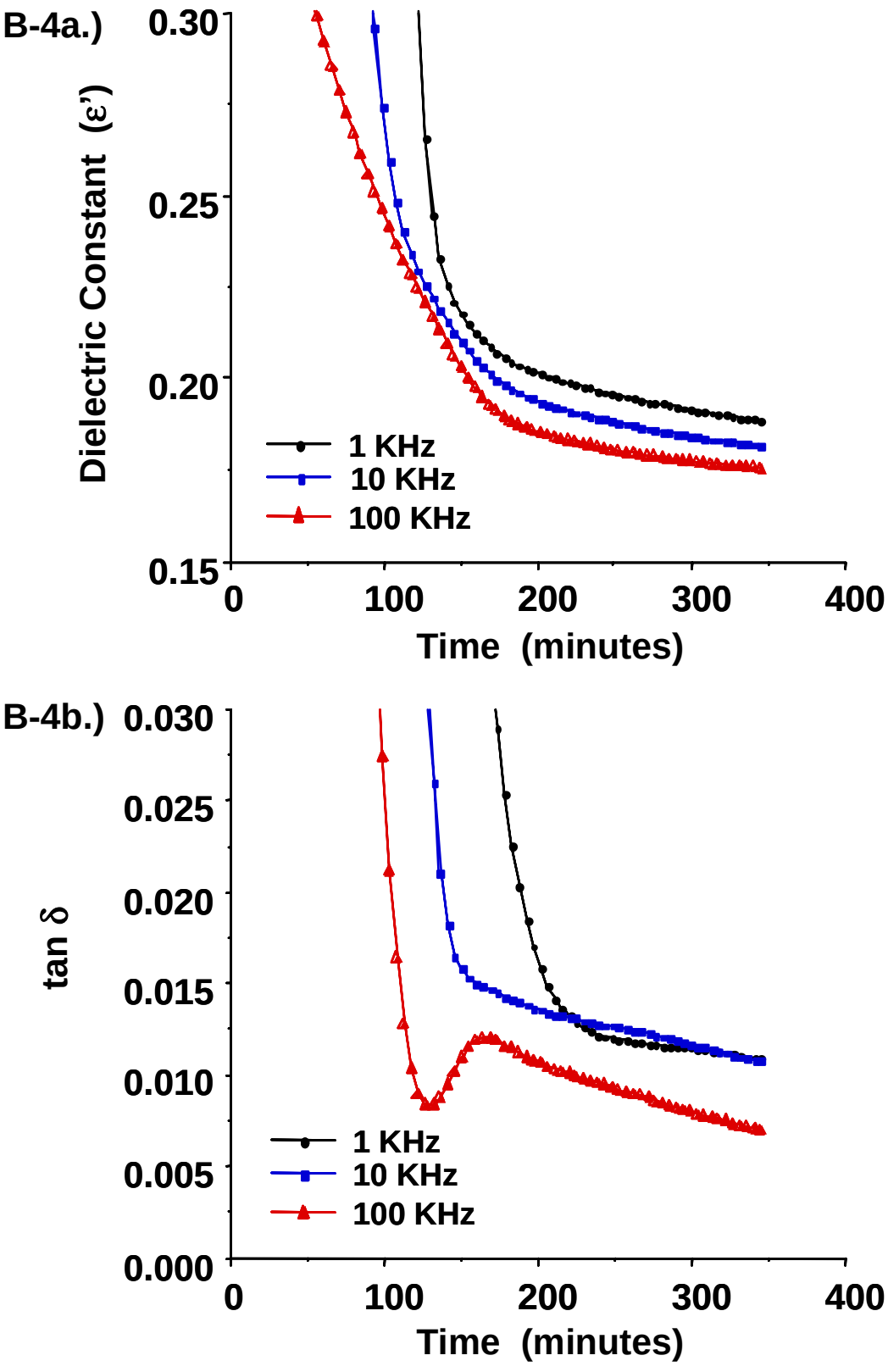

Figure B-4. Dipolar component to complex dielecric constant. Expanded Y-axis.
a.) Dielectric Constant vs. Time
b.) Tan δ vs. Time

By examining the findings of other researchers[B-14, B-20, B-21] and observing the glassy nature of the material at the end of the experiment, this longest cure time peak was assigned to vitrification of the material. It is evident from this data that the ionic and dipolar components of the complex dielectric constant are highly influenced by frequency. The next logical step was to examine the dependence of cure temperature on these properties.

Figure B-5 represents the tan δ data obtained from curing the unmodified cyanate ester material at three isothermal temperatures. Figure B-5a contains a comparison of the 1 kHz data, while Figure B-5b represents the data using the 100 kHz frequency. The first major difference observed in these data is that lower frequencies generate more sensitivity to ionic conductivity. This was manifested as a greater instrument signal at the lower frequencies. There also appears to be a dependence of the conductivity on temperature at higher frequencies. This is observed in Figure B-5b, where the material displays a higher initial tan δ value as temperature is increased. The 1 kHz data do not display such dependence. By expanding the tan δ axis, the temperature dependence of the vitrification is observed (Figure B-6). Temperature dependent vitrification peaks are clear in the high frequency data and again, suggest that dipolar alignment is dominant at higher frequencies and in highly viscous materials.

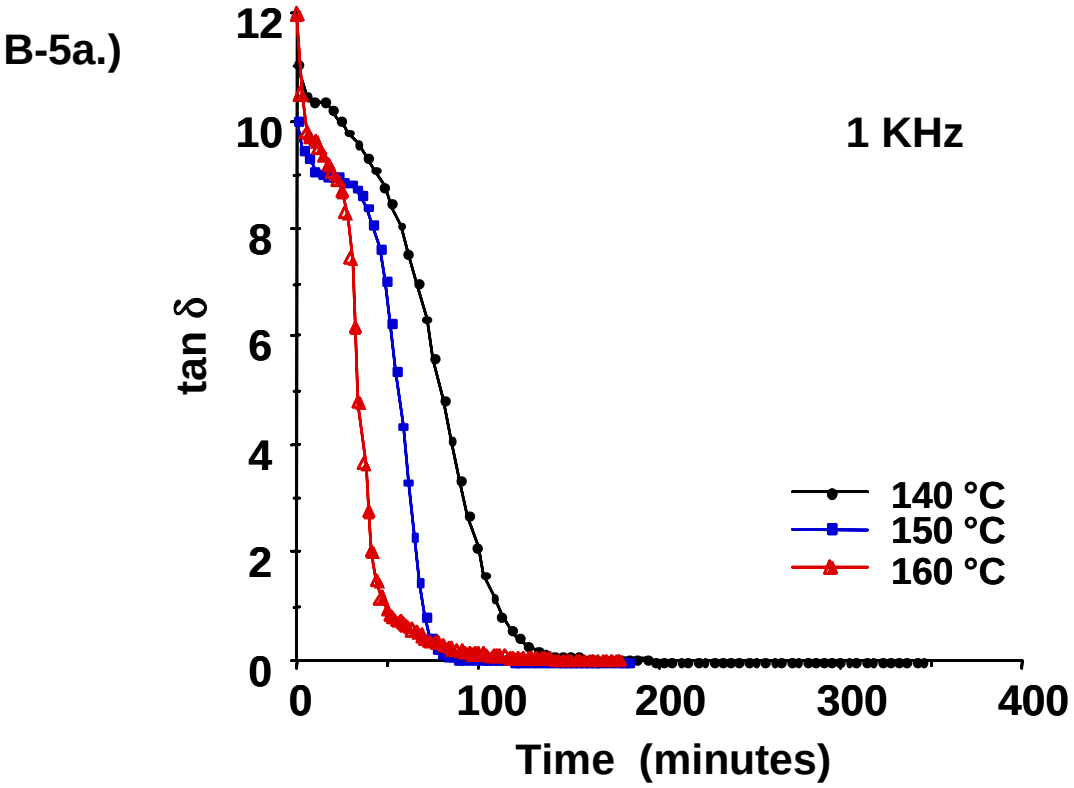

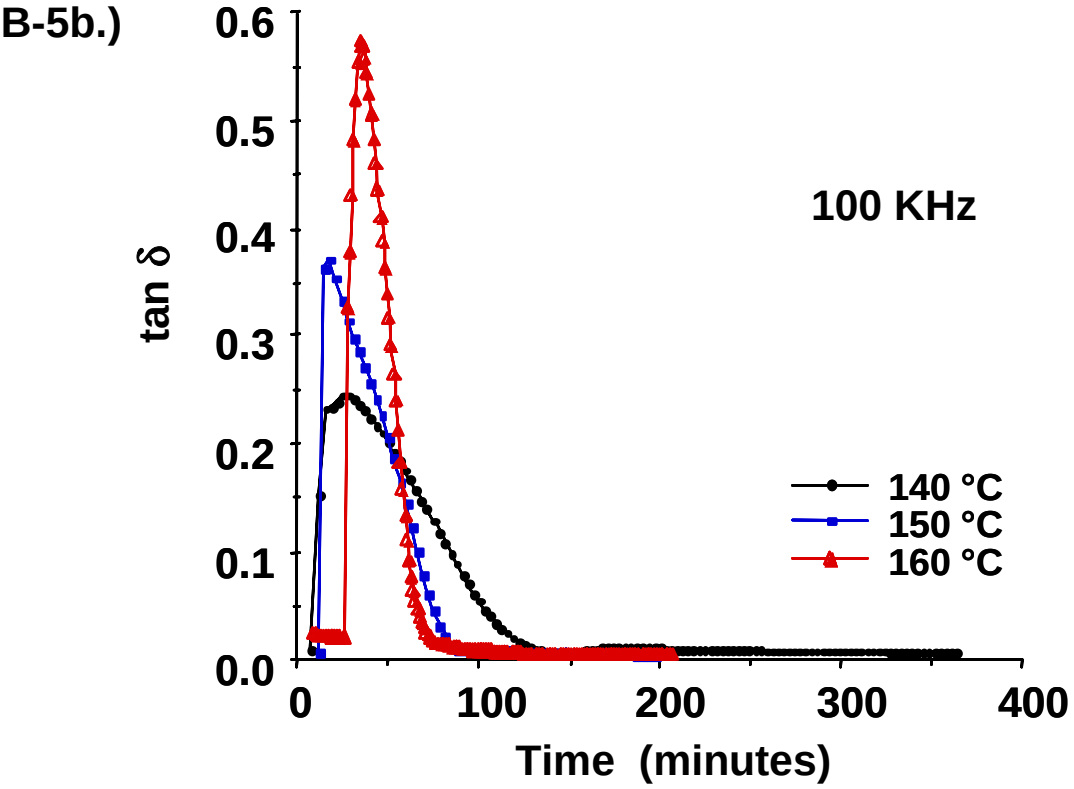

Figure B-5. Comparison of cure temperature on dielectric properties of an unmodified cyanate ester. Two frequency extremes represented.
a.) 1 KHz
b.) 100 KHz

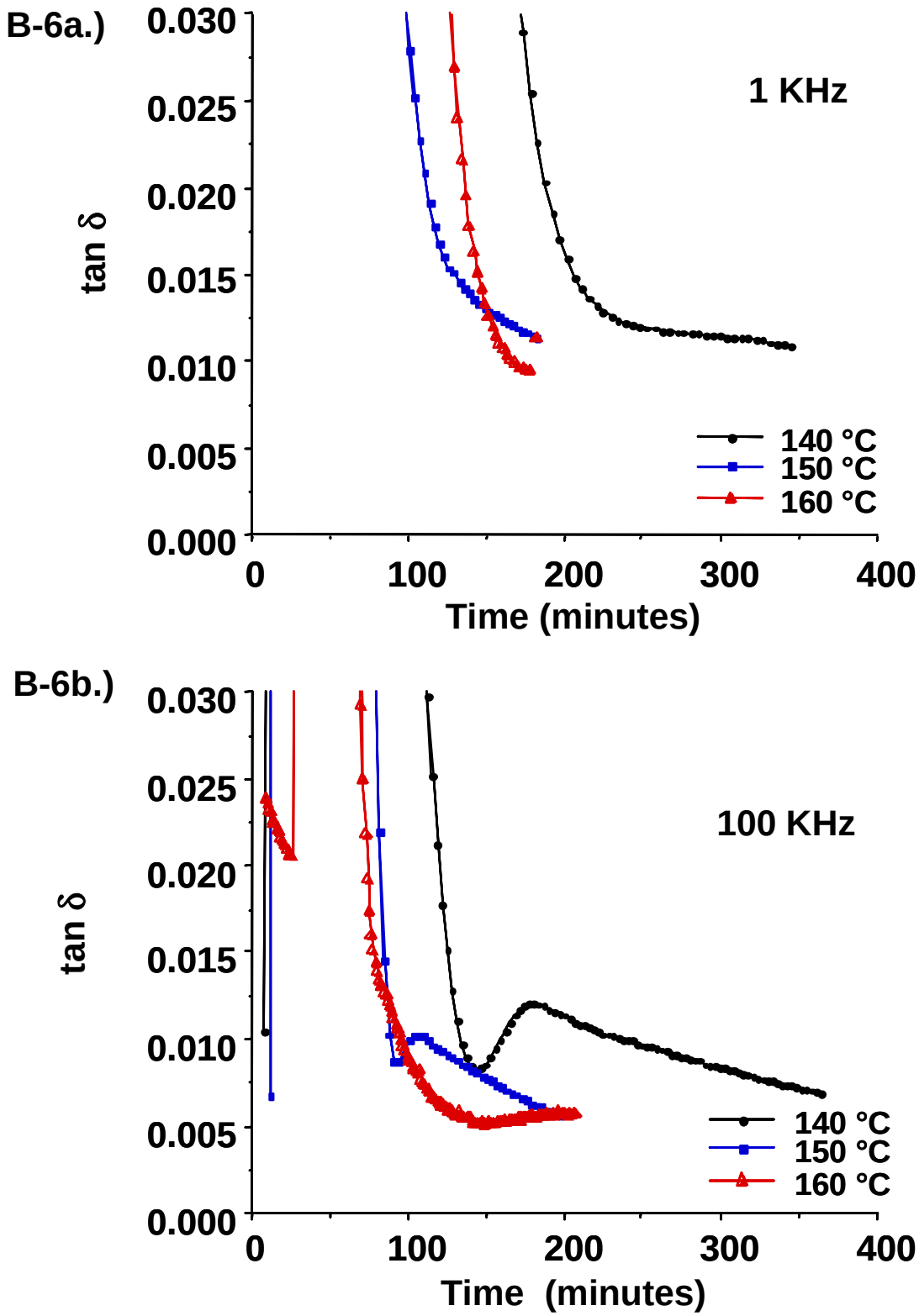

Figure B-6. Y-axis expansion of Figure B-5. Dipolar component comparison.

a.) 1 KHz

b.) 100 KHz

The principle that physical changes during the cure are detected earlier at higher applied frequencies is also observed (Figure B-6). Vitrification is clearly indicated in the higher frequency data, where in contrast, at lower frequencies it is not observed.

Since the cure properties of the unmodified cyanate ester were dependent on temperature and applied frequency, experiments were then performed on a thermoplastic modified cyanate ester resin, and the results compared. Figure B-7 contains a representative comparison using the dielectric constant of the unmodified and modified cyanate ester resins during cure at three isothermal cure temperatures. These data revealed the decrease in the dielectric constant of the modified thermoset during cure was less pronounced relative to the unmodified thermoset. Similar effects were observed in the isothermal melt viscosity data discussed previously (Figure A-7). Secondly, a shoulder appears which may be due to the incorporation of the thermoplastic toughener. This shoulder in the response occurs in the lower viscosity (conductivity dominant) region where gelation has not yet occurred, and is attributed to phase separation.

Examination of the dielectric tan δ data supports similar findings to those above (Figure B-8). The ionic conductivity is again the dominant factor early in the cure cycle (low initial viscosities). In the absence of the thermoplastic toughener, the intensity of the conductivity increases with temperature.

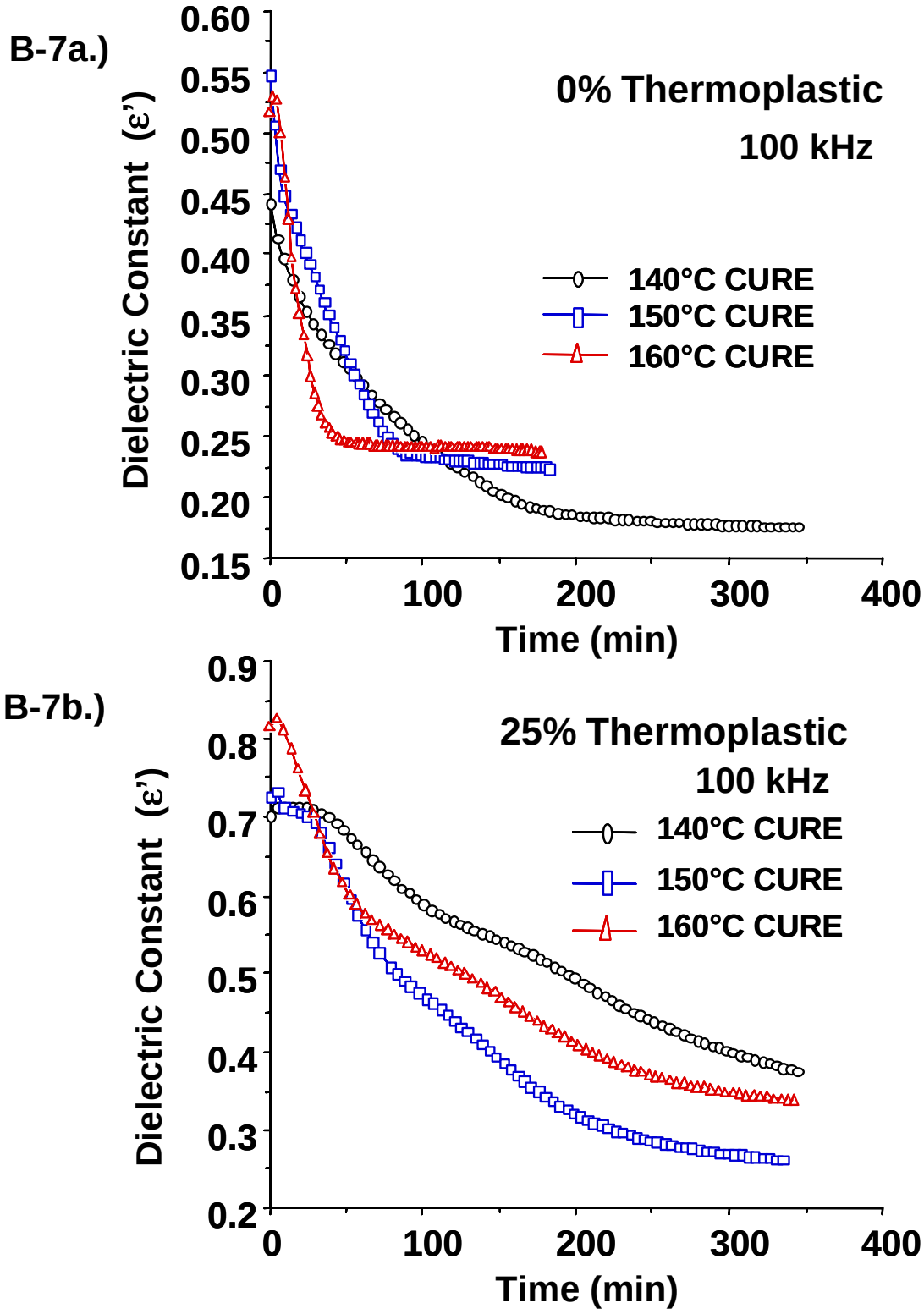

Figure B-7. Comparison of dielectric constant during cure of unmodified and modified cyanate ester resins.
a.) Neat Resin
b.) 25% Thermoplastic Toughened Resin

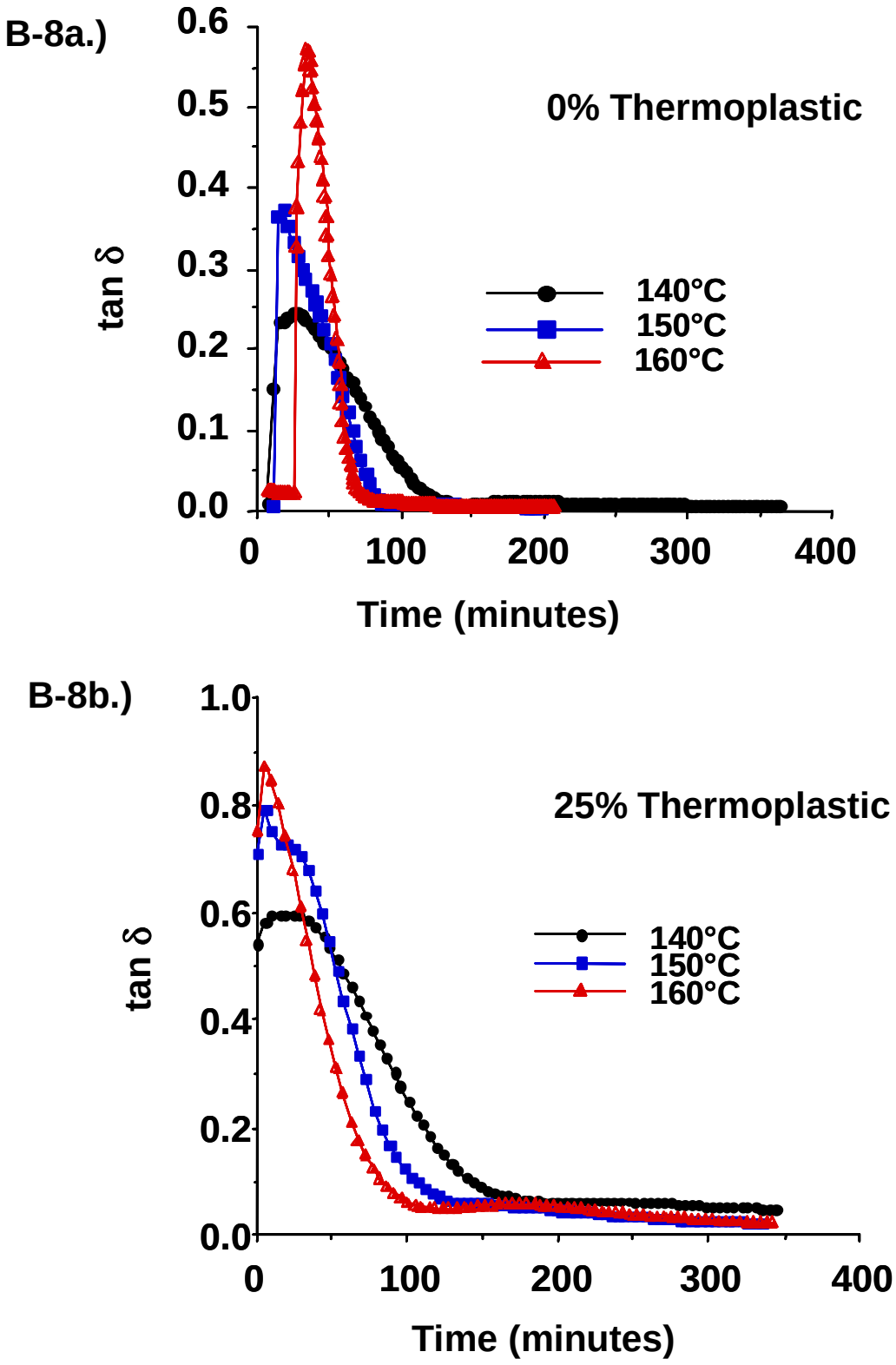

Figure B-8. Comparison of dielectric tan δ during cure of unmodified and modified cyanate ester resins.
a.) Neat Resin
b.) 25% Thermoplastic Toughened Resin

When the thermoplastic toughener is incorporated, little change in intensity is observed, and the decrease toward the dipolar region is broadened. Expanding the tan δ axis to examine the vitrification peak (Figure B-9) shows an increased response sensitivity of the modified cyanate ester material during this stage of the cure cycle. This suggests the thermoplastic toughener plays an important role in the cure of the cyanate ester thermoset. Further studies are required to separate or at least quantify this effect.

The goal of this thesis was to determine what properties could be measured on toughened thermosets from this dielectric remote sensor technique. Clearly, phase separation, gelation and vitrification are observable. The next step would logically be to determine the reproducibility of the measurements, perform tests over a broad temperature range, and construct a useful TTT diagram from the obtained data. These applications and expansions to the method are left for subsequent researchers.

B.4 SUMMARY & CONCLUSIONS

This study was designed to incorporate the use of dielectric remote sensors to examine the physical properties during cure of unmodified and thermoplastic toughener modified cyanate ester resins.

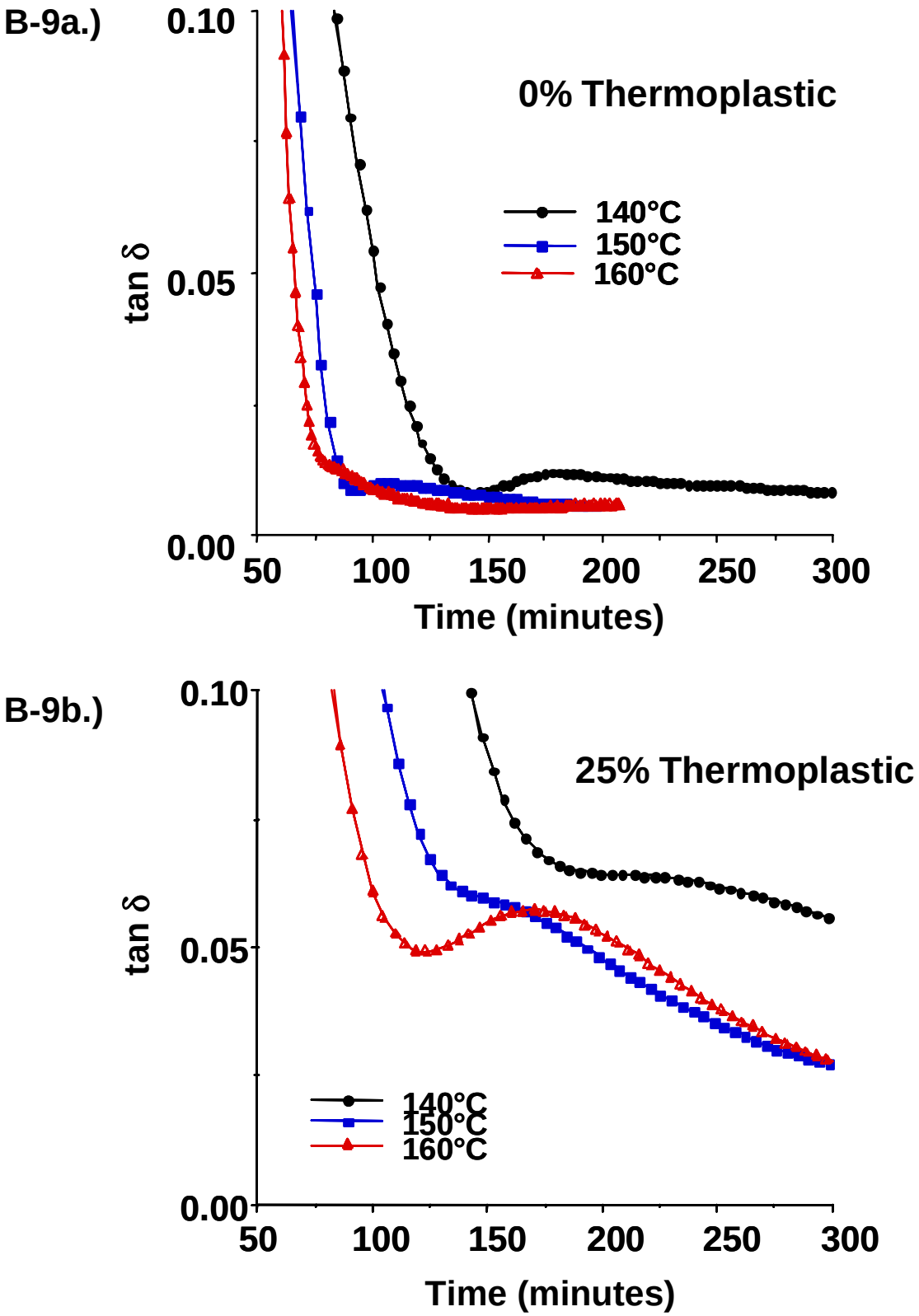

Figure B-9. Expansion of tan δ axis to observe vitrification peak. Comparison of unmodified and modified cyanate ester.
a.) Neat Resin
b.) 25% Thermoplastic Toughened Resin

The data obtained from this technique correlated well with results observed in other materials using similar data collection methods. Gelation was observed as the ionic component of loss and storage modulus at the point where the ionic contribution was suppressed. Evidence of vitrification was seen as a small tan δ peak in the dipolar dominant region of cure. These properties were observed in both the unmodified and modified materials and are frequency and temperature dependent. Finally, phase separation was observed in the modified materials as a shoulder in the ionic conductivity dominant region and occurred prior to gelation.

B.5 REFERENCES

B-1. P. R. Ciriscioli, G. S. Springer, Int. SAMPE Symp. Exhib., **34**, 312 (1989).

B-2. S. D. Senturia, N. F. Sheppard, Jr., H. L. Lee, S. B. Marshall, SAMPE Int'l. Symp., **28**, 851 (1983).

B-3. S. S. Chang, F. I. Mopsik, D. L. Hunston, SAMPE National Tech. Conf., **19**, 253 (1987).

B-4. D. R. Day, SAMPE Int'l. Symp., **33**, 594 (1988).

B-5. D. R. Day, SAMPE Int'l. Symp., **32**, 1472 (1987).

B-6. D. R. Day, SAMPE Int'l. Symp., **31**, 1095 (1986).

B-7. D. R. Day, T. J. Lewis, H. L. Lee, S. D. Senturia, J. of Adhesion, **18**, 73 (1985).

B-8. D. E. Kranbuehl, S. E. Delos, E. Yi, J. Mayer, T. Hou, W. Winfree, SAMPE Int'l. Symp., **30**, 638 (1985).

B-9. D. E. Kranbuehl, S. E. Delos, P. K. Jue, Polymer, **27**, 11 (1986).

B-10. D. E. Kranbuehl, P. Haverty, M. Hoff, R. D. Hoffman, J. J. Godfrey, 42nd Annual Conf., Comp. Institute, Soc. Plast. Industry, **Sess. 22-D**, 1 (1987).

B-11. D. E. Kranbuehl, et al., SAMPE Int'l. Symp., **32**, 338 (1987).

B-12. D. E. Kranbuehl, M. Hoff, P. Haverty, A. Loos, T. Freeman, SAMPE Int'l. Symp., **33**, 1276 (1988).

B-13. P. R. Ciriscioli, G. S. Springer, Int. SAMPE Symp. Exhib., **34**, 312 (1989).

B-14. M. A. Zumbrum, Ph.D Dissertation, Virginia Tech, 1990.

B-15. C. R. Lin, P. Y. Hsieh, SAMPE Int'l. Symp., **35**, 1233 (1990).

B-16. *Polymer-Polymer Miscibility*, O. Olabisi, L. M. Robeson, M. T. Shaw, Academic Press, NY, 1979.

B-17. D. R. Day, D. D. Sheppard, J. Coat. Technol., **60**, 57 (1988).

B-18. G. M. Maistros, H. Block, C. B. Bucknall, I. K. Partridge, Polymer, **33**, 4470 (1992).

B-19. A. J. MacKinnon, S. D. Jenkins, P. T. McGrail, R. A. Pethrick, Macromolecules, **25**, 3492 (1992).

B-20. "*Principles of Dielectrometry*", Micromet Technical Brochure.

B-21. D. E. Kranbuehl, Polym. Prepr. (Am. Chem. Soc. Div. Polym. Chem.), **31**, 289 (1990).

B-22. G. Banhegy, P. Hedvig, S. Petrovic, F. E. Karasz, Polym. Plast. Tech. Eng., **30**, 183 (1991).

B-23. D. R. Day, D. D. Sheppard, A. S. Wall, SAMPE Int'l. Symp., **33**, 603 (1988).

B-24. J. M. Brown, Ph.D Dissertation, Virginia Tech, 1994.

VITA

Daniel Robert Hahn was born on January 6, 1966 and raised in Akron, Ohio. He graduated high school in 1984 and went directly to college at the University of Akron, majoring in Chemistry. He received his B.S. degree in Chemistry in May 1989 after spending 1 year as a Co-Op student at Mead Imaging in Dayton, Ohio. Upon graduation, he went to Virginia Tech to work on his Ph.D. in Chemistry. After completing his research in the fall of 1995, he went to work for Tektronix in Wilsonville, Oregon. In May 1999, he successfully defended his research dissertation and completed his degree in May 2004. He now works as a research scientist for Xerox Corporation, formerly Tektronix, in Wilsonville, Oregon and lives in beautiful Hubbard, Oregon.